

Quark and Lepton Masses in 5D SO(10)

Hyung Do Kim^{a,b}, Stuart Raby^a and Leslie Schradin^a

^a*Department of Physics, The Ohio State University,*

174 W. 18th Ave., Columbus, Ohio 43210, USA

^b*School of Physics, Seoul National University,*

Seoul, 151-747, Korea

E-mail: hdkim@phya.snu.ac.kr

raby,schradin@mps.ohio-state.edu

ABSTRACT: We construct a five dimensional supersymmetric $SO(10) \times D_3$ grand unified model with an $S^1 / (Z_2 \times Z'_2)$ orbifold as the extra dimension. The orbifold breaks half of the supersymmetry and breaks the $SO(10)$ gauge symmetry down to $SU(4)_C \times SU(2)_L \times SU(2)_R$. The Higgs mechanism is used to break the remaining gauge symmetry the rest of the way to the Standard Model. We place matter fields variously in the bulk and on the orbifold fixed points and the resulting massless fields are mixtures between these brane and bulk fields. A chiral adjoint field in the bulk gets a $U(1)_X$ vacuum expectation value, resulting in an X -dependent localization of the bulk matter fields and the Standard Model Higgs field. This Higgs field localization allows us to simultaneously explain the hierarchies $m_u < m_d$ and $m_t \gg m_b$. The model uses 11 parameters to fit the 13 independent low energy observables of the quark and charged lepton Yukawa matrices. The model predicts the values of two quark mass combinations, $\frac{m_u}{m_c}$ and $m_d m_s m_b$, each of which are predicted to be approximately 1σ above their experimental values. The remaining observables are successfully fit at the 5% level. We note that this 5D theory, as formulated, has problems retaining the Pati-Salam Yukawa symmetry relations. A simple 6D fix, which preserves the 5D results, solves this problem.

KEYWORDS: SO(10) Unification, Extra Dimension, Fermion Mass.

Contents

1. Introduction	1
2. Data	6
3. Setup	9
3.1 Background	9
3.2 Yukawa Matrix	14
4. Analysis	20
4.1 Analytic Fitting	21
4.2 Numerical Fitting	29
5. Justification in 6D	32
6. Summary and Discussion	36
A. D_3 Family Symmetry	37
B. Massless States and Wavefunctions	39
C. A Lifted 4D Model	40

1. Introduction

The Standard Model (SM) of particle physics has had spectacular success in describing the strong, weak, and electromagnetic forces of nature in terms of gauge theory. It does, however, leave several issues unexplained. Among these issues: First, in the Standard Model the three gauge coupling values are arbitrary and unrelated, but appear to almost unify at a high scale. The assumption of supersymmetry improves this unification. Second, the fermion charge assignments under the gauge symmetries are arbitrary. Third, recent experiments have shown that neutrinos have masses, but they are massless in the Standard Model. Fourth, in a universe initially balanced between

matter and anti-matter, interactions which violate baryon number are required to explain the apparent baryon asymmetry observed in the universe. Baryon number is conserved by the renormalizable terms of the Standard Model. Fifth, the weak and Planck scales are 16 orders of magnitude apart, causing a naturalness problem in the mass of the Higgs boson. While this is not an exhaustive list of problems with the Standard Model, all of these issues are addressed by four dimensional supersymmetric grand unified theories [4D SUSY GUTS] [1, 2, 3, 4, 5, 6].

In a SUSY GUT, the three gauge couplings meet near the GUT scale $M_G \simeq 3 \times 10^{16}$ GeV, and above this scale an enlarged symmetry group with a single gauge coupling governs physics. Within this paper, we will take SO(10) as our gauge group. Remarkably, the charges of the SM fermions are exactly those which come from a 16 of SO(10), including the arbitrary (in the SM) $U(1)_Y$ hypercharge quantum numbers. Moreover, a 16 dimensional representation requires the addition of a sterile neutrino which can lead to tiny neutrino masses through a See-Saw mechanism. $B - L$ is a gauge symmetry within SO(10) which is broken at a high scale in the unified theory, thus making Baryogenesis possible. Finally, the presence of supersymmetry near the weak scale gives a natural explanation for a Higgs mass at that scale.

As experiments become more accurate, we are able to test whether GUT theories work in their minimal forms. There are several indications that the most simple GUT theories cannot work.

- With the definition of the GUT scale M_G : $\alpha_1(M_G) \equiv \alpha_2(M_G) \equiv \alpha_{\text{GUT}}$, the assumption of exact unification ($\alpha_3(M_G) = \alpha_{\text{GUT}}$) leads to a prediction for $\alpha_3(M_Z)$ which is larger than the measurements. This indicates that a negative threshold correction to α_3 must be present at the GUT scale: $\varepsilon_3 \equiv \frac{\alpha_3(M_G) - \alpha_{\text{GUT}}}{\alpha_{\text{GUT}}} \simeq -0.04$ [7].
- Since the fermions are combined into fewer multiplets of the unifying group, GUT theories in general give relationships between the fermion masses at the GUT scale. In SO(10), third family unification can be accommodated ($m_\tau(M_G) = m_b(M_G) = m_t(M_G)$), but the first and second family masses do not unify at M_G . The Georgi-Jarlskog relation: $m_s/m_\mu = \frac{1}{3}m_b/m_\tau$ [8], which had been known to work very well, holds less well as measurements of the strange quark mass decrease.
- GUT models place the weak Higgs doublet(s) into larger representations which include new color triplet Higgs fields. It is difficult to make the color triplets heavy enough (near GUT scale mass) to avoid rapid proton decay while keeping the weak doublets light (weak scale mass). The doublet-triplet (DT) splitting

problem is related to the method by which the GUT symmetry is broken to the Standard Model, and the models which give proper DT splitting can be quite complicated.

Orbifold GUTS have been considered extensively for the last five years [9, 10, 11, 12, 13, 14, 15, 16, 17, 18, 19] and provide answers to some of the above issues. If the compactification radius is slightly smaller than the cutoff scale, the heavy Kaluza-Klein (KK) modes can give compactification scale threshold corrections necessary for exact gauge unification at the cutoff scale [20]. If the Standard Model Higgs is a bulk field, and if the triplet Higgs has twisted boundary conditions under the orbifold it will acquire a mass at the compactification scale, thus solving the DT splitting problem naturally. The same mechanism breaks the GUT gauge symmetry and gives mass to gauge bosons outside of the Standard Model.

5D SU(5) models have a SM brane on which all of the interesting GUT mass relations are absent. The first and second family matter fields usually feel this brane and so there are no relations between quarks and leptons in these two families. This is unattractive since the models lose predictivity. For this reason, we choose to concentrate on SO(10) models which give more possible avenues of symmetry breaking to the Standard Model and allow for GUT mass relations.

5D SO(10) SUSY GUTS were first considered in Dermisek and Mafi [18], and a setup which gives gauge coupling unification was constructed by Kim and Raby [20]. The extra dimension is an $S^1/(Z_2 \times Z_2')$ orbifold, a line segment with endpoints which are fixedpoints of the orbifold Z_2 symmetries. 5D N=1 SUSY is broken to 4D N=1 by the first Z_2 , while the second Z_2 breaks SO(10) to SO(6) \times SO(4) (= SU(4) \times SU(2) \times SU(2) \equiv Pati-Salam gauge group). Further breaking to the Standard Model is provided by the Higgs mechanism on one of the fixed points. One fixed point, the SO(10) brane, is invariant under the first Z_2 and has SO(10) gauge symmetry. The other fixed point, the Pati-Salam (PS) brane, is invariant under the second Z_2 and only has Pati-Salam gauge symmetry. The bulk has the full SO(10) gauge symmetry. Gauge coupling unification works if the compactification scale is approximately 10^{14} GeV, the cutoff scale is approximately 10^{17} GeV, and if the Higgs multiplet lives in the bulk. A virtue of the model is that SO(10) or Pati-Salam exists after the orbifold breaking and we retain some of the Yukawa GUT relations.

We note that there is a problem with the five dimensional formulation of our theory. In order for the gauge couplings to unify at the cutoff scale, the PS brane fields breaking Pati-Salam down to the Standard Model must have cutoff-scale VEVs. Therefore, in general one would expect all aspects of PS symmetry to be broken at this high scale, and that the lower-energy theory should not be expected to exhibit PS symmetry.

Nevertheless, we wish to retain some of the PS symmetry below the cutoff scale in order to preserve the PS Yukawa coupling relations. This is possible if there is an additional extra dimension in which the PS brane is separated from the PS-breaking VEV fields. This 6th direction will solve this problem if its length scale is only slightly larger than the cutoff scale. The effective 5D theory below the energy scale of this 6th direction will not be affected in any other way. For this reason we choose to perform our analysis in the 5D theory, and will assume that PS Yukawa relations are still valid below the cutoff-scale. We discuss the 6D fix to the PS-breaking problem in Section 5.

Attempts to explain the mass hierarchy between the different families of fermions have often centered on flavor symmetries. There are models based on abelian horizontal U(1) symmetries where the smallness of certain couplings is explained by the suppression given by high powers of U(1) breaking fields. The explanations can at most be qualitative as there are order one coefficients which are undetermined from the U(1) symmetry. We therefore choose to concentrate on non-abelian flavor symmetry. With three families, the largest possible symmetry would be SU(3). However, the order one top Yukawa coupling would badly break the SU(3) symmetry, and so instead we choose to concentrate on an SU(2) symmetry between the first two families. This symmetry can explain the absence of flavor changing neutral currents in supersymmetric theories and can relate unknown order one coefficients between different families. In string theory, global symmetries are thought to be generally broken by quantum gravity effects [21, 22, 23], and so our flavor symmetry should be a gauge symmetry. However, the breaking of a continuous gauge symmetry like SU(2) gives unwanted flavor changing neutral currents from the D-term contributions [24, 25]. For this reason, we assume a flavor symmetry relating the first and second families based on D_3 , a discrete subgroup of SU(2). As a discrete gauge symmetry, D_3 has all the virtues of SU(2) and can avoid the problem related to continuous gauge symmetry [26]. More information and references on family symmetries in grand unified theories can be found in the reviews [27, 28, 29].

In SUSY SO(10) models with flavor symmetries, the most difficult thing to explain is why $m_u < m_d$ while $m_t \gg m_b$. In SO(10) models, we usually have $m_t/m_b = Y_t/Y_b \tan \beta \sim \tan \beta$, and the heaviness of the top quark is explained by a large value for $\tan \beta \sim 50$. In these models, it is natural that $Y_u/Y_d \sim Y_t/Y_b$, which leads to $m_u/m_d \sim 50$. To fit the data, an unusually small Yukawa coupling is needed for the up quark compared to the down quark. This is difficult to implement in SO(10) models. Extra-dimensional theories provide a nice tool to suppress or enhance fermion masses, as the size of a mass can be influenced by the localization of the matter and Higgs fields within the extra dimension. Others, notably Arkani-Hamed and Schmaltz in [30], have used localization in an extra dimension to explain the fermion mass hierarchy. Our

model, on the other hand, retains some of the attractive Yukawa relations present in 4D GUT models which are not present in [30].

We explain the ratios $m_u/m_d < 1$ and $m_t/m_b \gg 1$ simultaneously by the quasi-localization of the Higgs field in the bulk by a kink mass.¹ We give a vacuum expectation value (VEV) in the $U(1)_X$ direction to a scalar adjoint field Σ contained in the 5D vector multiplet. Σ is odd under both Z_2 parities, and we choose the VEV so that its contribution to the D-term VEV is only at the two branes. Supersymmetry can be preserved if there are fields on each brane which get VEVs in the right-handed neutrino direction to counter the contribution of $\langle \Sigma \rangle$ to the D-term VEV. The VEV of Σ acts to give a $U(1)_X$ -dependent mass to the hypermultiplet fields in the bulk, in particular the Higgs field. Because H_u and H_d carry opposite $U(1)_X$ charges, they are localized towards different branes. Thus if the 1st and 3rd families get their Yukawa couplings on opposite branes, we can naturally have $m_u/m_d < 1$ and $m_t/m_b > 1$.

The easiest way to ensure that the 1st and 3rd families get their Yukawa couplings on opposite branes is to restrict them to these branes. By proton decay constraints, the 1st family cannot reside on the $SO(10)$ brane. Thus we choose the 1st (and by family symmetry, the 2nd) family to be on the PS brane, and the 3rd family to be on the $SO(10)$ brane. We then choose the sign of the kink mass VEV to be such that H_u is localized towards the $SO(10)$ brane and H_d is localized towards the PS brane.² Communication between the first two families and the third is provided by mixing with bulk fields. After requiring that the 1st and 3rd families be brane fields, the location of the Higgs and all matter fields is entirely determined from gauge coupling unification, proton decay constraints, D_3 family symmetry between the first two families, and the action of the kink mass to explain 1st and 3rd family mass ratios.

To summarize: In this paper, we construct a 5D $SO(10)$ supersymmetric orbifold GUT model in which the 1st and 2nd families reside on the PS brane and transform as a doublet under the D_3 family symmetry, the 3rd family is located on the $SO(10)$ brane, and a kink mass localizes the MSSM Higgs doublets to opposite sides of the bulk. The model explains the 13 independent quark and charged lepton masses and mixing angles in terms of 11 parameters. The two predictions are $\frac{m_u}{m_c}(M_Z) = 0.0037 \pm 0.0006$ and

¹The extreme limit is discussed in [31] where H_u is on the brane and H_d is in the bulk such that $m_t \gg m_b$ for order one $\tan \beta$.

²These arguments do not rule out the case of all 3 families in the bulk, or some fields on branes with others in the bulk. However, if the 3rd family is a brane field, then the 2nd family must also be a brane field or the ratio $\frac{m_\mu}{m_\tau}$ is made too small by volume suppression to fit the data. It is possible to decrease the suppression from the volume factor by either placing only half of the 2nd family in the bulk and/or by altering the GUT threshold correction ε_3 . We made some attempts with these approaches but were unable to produce viable theories.

$m_d m_s m_b(M_Z) = (10.7 \pm 5.0) \times 10^5 \text{ MeV}^3$, both of which are approximately 1σ above the experimental values.

We lay out the remainder of this paper as follows. The data is summarized in Section 2. The basic setup is explained in Section 3. This includes background material and our choice of superpotential and Yukawa matrices. Section 4 contains the analysis of our data. This part is broken into two subsections: an analytic section (Section 4.1) giving predictions and approximate relationships between the model parameters and the data, and a numerical section (Section 4.2) with more precise results. The possibilities and advantages of placing our model in a 6D framework are given in Section 5. Finally, we present a summary and discussion of our model in Section 6. We also provide necessary information on D_3 family symmetry in Appendix A and a determination of massless state wavefunctions in Appendix B. Finally, in Appendix C we consider a 4D $SO(10)$ SUSY GUT model [32] lifted up to 5D. In this model the smallness of the up quark mass is explained by an approximate left-right (LR) symmetry rather than by a kink VEV.

2. Data

In this section we tabulate the low energy data used in our analysis. First the data associated with the Cabbibo-Kobayashi-Maskawa (CKM) matrix. These CKM elements we take from [33].

$$\begin{aligned} |V_{us}| &= 0.2240 \pm 0.0036 & (2.1) \\ |V_{cb}| &= (41.5 \pm 0.8) \times 10^{-3} \\ \left| \frac{V_{ub}}{V_{cb}} \right| &= 0.086 \pm 0.008 \end{aligned}$$

$|V_{td}|$ and $\sin 2\beta$ we take from [34].

$$\begin{aligned} |V_{td}| &= 0.0082 \pm 0.0008 & (2.2) \\ \sin 2\beta &= 0.739 \pm 0.048 \end{aligned}$$

We use [35] for J and ε_K .

$$\begin{aligned} J &= (3.0 \pm 0.3) \times 10^{-5} & (2.3) \\ \varepsilon_K &= (2.282 \pm 0.017) \times 10^{-3} \end{aligned}$$

Next the low energy quark mass observables. We use

$$Q \equiv \frac{\frac{m_s}{m_d}}{\sqrt{1 - \left(\frac{m_u}{m_d}\right)^2}} \quad (2.4)$$

and m_s/m_d from [36] with doubled errors on m_s/m_d , the unquenched lattice QCD result with $n_f = 2$ for m_s [37] with doubled errors, and we take the quenched lattice QCD result for m_c with 10% error from [33] and double the error. We use the bottom quark mass from [38] and the top quark pole mass from the CDF and DØ Collaboration [39].

$$\begin{aligned}
Q &= 22.7 \pm 0.8 & (2.5) \\
\frac{m_s}{m_d} &= 18.9 \pm 0.8 \times 2 \\
m_s(2 \text{ GeV}) &= 89 \pm 11 \times 2 \text{ MeV} \\
m_c(m_c) &= 1.30 \pm 0.15 \times 2 \text{ GeV} \\
m_b(m_b) &= 4.22 \pm 0.09 \text{ GeV}. \\
M_t(\text{pole}) &= 178.0 \pm 4.3 \text{ GeV} \\
m_t(m_t) &= 169 \pm 4 \text{ GeV}
\end{aligned}$$

In our analysis, we will calculate our observables at the energy scale M_Z , except for the top mass for which we will use $m_t(m_t)$. Therefore we need to convert our data to values at M_Z . Define the running parameters:

$$\eta_i \equiv \begin{cases} \frac{m_i(M_Z)}{m_i(m_i)} & \text{for } i = c, b \\ \frac{m_i(M_Z)}{m_i(2 \text{ GeV})} & \text{for } i = u, d, s. \end{cases} \quad (2.6)$$

At two loops in QCD we find

$$\begin{aligned}
\eta_c &= 0.56, & \eta_b &= 0.69, & (2.7) \\
\eta_u &= \eta_d = \eta_s = 0.65.
\end{aligned}$$

The lepton masses at M_Z from [40] are

$$\begin{aligned}
m_e &= 0.48684727 \pm 0.00000014 \text{ MeV} & (2.8) \\
m_\mu &= 102.75138 \pm 0.00033 \text{ MeV} \\
m_\tau &= 1746.7 \pm 0.3 \text{ MeV}.
\end{aligned}$$

Also from [40], we take the gauge couplings at M_Z :

$$\begin{aligned}
\alpha_1(M_Z) &= 0.016829 \pm 0.000017 & (2.9) \\
\alpha_2(M_Z) &= 0.033493 \pm 0.000059 \\
\alpha_3(M_Z) &= 0.118 \pm 0.003
\end{aligned}$$

We use the mass of the Z-boson to set the weak energy scale: [35]

$$M_Z = 91.1876 \pm 0.0021 \text{ GeV} \quad (2.10)$$

In our model, we do not calculate the effects of electro-weak symmetry breaking. We assume that it happens properly and gives the correct weak scale masses. For this reason, we use a calculated Higgs VEV at M_Z .

$$\begin{aligned} v &= \frac{M_Z}{\sqrt{\pi} \sqrt{\frac{3}{5} \alpha_1(M_Z) + \alpha_2(M_Z)}} \\ &= 246.41 \pm 0.17 \text{ GeV} \end{aligned} \quad (2.11)$$

Additional information is needed to calculate ε_K in our model. We use the CKM parametrization-independent formula

$$|\varepsilon_K| = \frac{C_\varepsilon}{2} B_K \left[\text{Im} \left(\frac{(\square_c)^2}{\square_u} \right) S_c \sigma_c + \text{Im} \left(\frac{(\square_t)^2}{\square_u} \right) S_t \sigma_t + 2 \text{Im} \left(\frac{\square_c \square_t}{\square_u} \right) S_{ct} \sigma_{ct} \right] \quad (2.12)$$

where

$$\square_i \equiv V_{ud} V_{us}^* V_{is} V_{id}^* \quad (2.13)$$

and the various S_i functions are Inami-Lim functions [41]. The σ_i are $\mathcal{O}(1)$ factors which we take from Battaglia [33]

$$\sigma_c = 1.32 \quad \sigma_t = 0.57 \quad \sigma_{ct} = 0.47. \quad (2.14)$$

C_ε is a ratio of well known low-energy observables. From Battaglia [33], this combination is

$$C_\varepsilon = \frac{G_F^2 f_{K^+}^2 m_{K^0} M_W^2}{6\pi^2 \sqrt{2} \Delta m_K} = 3.837 \times 10^4. \quad (2.15)$$

We neglect the error associated with C_ε since it is small and will not affect the theoretical error in ε_K . A large part of this theoretical error comes from B_K for which we use [33].

$$\begin{aligned} B_K &= 0.86 \pm 0.06 \pm 0.14 \\ &\simeq 0.86 \pm 0.15 \end{aligned} \quad (2.16)$$

where in the last line we add the statistical and systematic errors in quadrature.

3. Setup

3.1 Background

We consider a five dimensional supersymmetric SO(10) GUT compactified on an $S^1/(Z_2 \times Z'_2)$ orbifold where S^1 is described by $y \in [0, 2\pi R]$. The first orbifold, Z_2 , under which $y \rightarrow -y$, breaks 5D N=1 supersymmetry (4D N=2) to 4D N=1. The other orbifold, Z'_2 , under which $y \rightarrow -y + \pi R$, breaks SO(10) down to the PS gauge group $SU(4)_C \times SU(2)_L \times SU(2)_R$. The fundamental domain of the y direction is the line segment $y \in [0, \pi R/2]$. SO(10) gauge symmetry is present everywhere except at the point $y = \pi R/2$, which only has Pati-Salam gauge symmetry. Hence, we call the two inequivalent fixed points the ‘‘SO(10)’’ ($y = 0$) and ‘‘Pati-Salam’’ branes ($y = \pi R/2$) where each fixed point is a three-brane (3+1 dimensional spacetime). The Higgs mechanism on the PS brane completes the breaking of the PS gauge symmetry to the SM gauge group.

The fields which live in the five dimensional space between the branes (known as the ‘‘bulk’’) are even or odd under the orbifold parities. We denote the parity of a given field under these orbifolds by two \pm subscripts on the field with the first corresponding to Z_2 and the second corresponding to Z'_2 . This part of the setup, including the orbifold structure, field parities, and supersymmetry and gauge symmetry breaking are based on work done in [18] and [20]. For more details, please see these references.

We wish to relate some of our fields by a family symmetry, D_3 , under which the first and second family fields form a doublet. Other fields within our model will be in various representations of D_3 which will affect the structure of the Yukawa matrices we generate. We take the family symmetry to be independent of the orbifold symmetries. A brief summary of the D_3 group is provided in Appendix A, where we give the information necessary to understand the family representations and couplings used in our model. For more information, see the Appendix presented in [32].

The 5D supersymmetric vector multiplet $\mathcal{V} = (A_M, \lambda_1, \lambda_2, \Sigma)$ contains a 4D vector multiplet $V = (A_\mu, \lambda_1)$ and a 4D chiral adjoint $\phi = ((\Sigma + iA_5)/\sqrt{2}, \lambda_2)$. For a generic hypermultiplet $\mathcal{H} = (h, \bar{h}, \psi, \bar{\psi})$ which breaks up into the 4D chiral multiplets $\Phi = (h, \psi)$ and $\bar{\Phi} = (\bar{h}, \bar{\psi})$, we use Arkani-Hamed et. al. [42] for the 5D action:

$$S \supset \int d^4x dy \left\{ \int d^4\theta \left[\bar{\Phi} e^V \Phi^\dagger + \Phi^\dagger e^{-V} \Phi \right] + \left[\int d^2\theta \bar{\Phi} \left(m + \partial_y - \frac{1}{\sqrt{2}} \phi \right) \Phi + \text{h.c.} \right] \right\} \quad (3.1)$$

The mass m refers to the mass of the 5D fields, which we set to zero for all hypermultiplets. We take the field Σ ($\subset \phi$) to get a VEV in the X direction of SO(10). Because

of the coupling in the action:

$$\begin{aligned}
S &\supset \int d^4x dy \int d^2\theta \bar{\Phi}(\partial_y - \frac{1}{\sqrt{2}}\phi)\Phi \\
&\xrightarrow{\text{VEV}} \int d^4x dy \int d^2\theta \bar{\Phi}(\partial_y - m_X)\Phi
\end{aligned} \tag{3.2}$$

this VEV will generate X -dependent masses m_X for the bulk chiral fields coming from hypermultiplets in the theory. The $U(1)_X$ of $SO(10)$ is contained inside Pati-Salam, and the chiral adjoint for PS has $(--)$ parity. Therefore the mass m_X we have generated also has this odd-odd parity under the orbifold. For this reason we call it a kink mass.

The D-term for this theory is

$$D = -(\partial_y \Sigma + i[\Sigma, A_5]), \tag{3.3}$$

hence a VEV of Σ is potentially dangerous since it could create a D-term VEV. To avoid this, we take $\langle \Sigma \rangle$ to be flat in the bulk with discontinuities at the branes to be consistent with its $(--)$ parity. These discontinuities generate D-term VEVs on the branes, but we can choose to add brane fields (16_{kink} on the $SO(10)$ brane, χ_{kink}^c and $\bar{\chi}_{\text{kink}}^c$ on the PS brane) with VEVs in the ν^c and $\bar{\nu}^c$ directions to cancel these effects from $\partial_y \langle \Sigma \rangle$, leaving us with a D-flat theory.³ More concretely, if the sterile sneutrino component of 16_{kink} (ν_{kink}^c) and the charge conjugate sterile sneutrino component of $\bar{16}_{\text{kink}}$ ($\bar{\nu}_{\text{kink}}^c$) get their VEVs, the D-flat condition for the $U(1)_X$ subgroup is given by

$$\partial_y \langle \Sigma \rangle = g^2 \left[5|\langle \nu_{\text{kink}}^c \rangle|^2 \delta(y) - 5|\langle \bar{\nu}_{\text{kink}}^c \rangle|^2 \delta(y - \frac{\pi R}{2}) \right]. \tag{3.4}$$

As ν_{kink}^c and $\bar{\nu}_{\text{kink}}^c$ carry only $U(1)_X$ charges, they do not appear in the D-term of the standard model gauge group. The D-flat condition is satisfied for

$$\langle \Sigma \rangle = \Sigma_0 \varepsilon_{--}(y), \tag{3.5}$$

$$|\langle \nu_{\text{kink}}^c \rangle|^2 = |\langle \bar{\nu}_{\text{kink}}^c \rangle|^2 = \frac{2\Sigma_0}{5g^2}. \tag{3.6}$$

ε_{-+} and ε_{--} are step functions on the orbifold. Both of these will be used later in our analysis.

$$\varepsilon_{-+}(y) \equiv \begin{cases} -1 & \text{for } y \in [-\pi R, 0] \\ +1 & \text{for } y \in [0, \pi R] \end{cases} \tag{3.7}$$

$$\varepsilon_{--}(y) \equiv \begin{cases} +1 & \text{for } y \in [-\pi R, -\frac{\pi R}{2}] \\ -1 & \text{for } y \in [-\frac{\pi R}{2}, 0] \\ +1 & \text{for } y \in [0, \frac{\pi R}{2}] \\ -1 & \text{for } y \in [\frac{\pi R}{2}, \pi R] \end{cases} \tag{3.8}$$

³This technique is described in [42] and used in [43].

We choose to parametrize the kink mass as follows:

$$m_X(y) = \varepsilon_{--}(y) X \frac{\Sigma_0}{2} = \varepsilon_{--}(y) X \frac{\zeta}{\pi R} \quad (3.9)$$

$$\zeta \equiv \frac{\Sigma_0 \pi R}{2}.$$

ζ will turn out to be a useful dimensionless parameter in later analysis.

If our $U(1)_X$ -breaking fields were to get VEVs as large as the cutoff scale, we could not keep $SO(10)$ or Pati-Salam as our symmetries on the branes. However, it turns out that $\zeta \sim 2$ is needed to fit the observed physical quantities, and so the corresponding VEVs are

$$\langle \nu_{\text{kink}}^c \rangle \sim \sqrt{\frac{8}{5\pi R g^2}} = \sqrt{\frac{16}{5\pi^2 g_4^2 R^2}} \sim \frac{1}{R}.$$

Therefore, all the VEVs necessary to give a kink mass are around the compactification scale and the breaking effects are suppressed at least by $M_c/M_* \sim 10^{-2}$ or 10^{-3} [20]. For the most part, the $U(1)_X$ breaking effects come from the kink profiles of bulk fields which are calculable and are exponentially proportional to the $U(1)_X$ charges. It is a novel example of obtaining large (order one) symmetry-breaking with a very small symmetry-breaking order parameter Σ . We stress that the VEVs of Σ , ν_{kink}^c and $\overline{\nu}_{\text{kink}}^c$ do not spoil the symmetries on the branes.

On the other hand, on the Pati-Salam brane gauge coupling unification requires χ^c and $\overline{\chi}^c$ to get VEVs of order the cutoff scale ($\overline{\chi}^c$ and χ^c are different from $\overline{\chi}_{\text{kink}}^c$ and χ_{kink}^c). This is a serious problem for our theory. There are order one corrections in the Kahler potential and Pati-Salam symmetry is badly broken in the canonical basis:

$$K = \left(1 + C \frac{\chi^{c\dagger} \chi^c}{M_*^2}\right) \psi^\dagger \psi \quad (3.10)$$

where C is of order one, $\langle \chi^c \rangle = \langle \chi^{c\dagger} \rangle \sim M_*$, and where ψ is a generic Pati-Salam brane field. This problem can be solved in a geometric way if there is a sixth dimension along which χ^c and ψ are separated. If this sixth dimension has a length scale R_2 slightly larger than the cutoff length scale, we can simultaneously retain the desired PS-brane Yukawa relations and gauge coupling unification. The 6D setup will be discussed in detail in section 5. Until then, we choose to concentrate on the effective 5D theory below this 6D scale. The 5D analysis of the Yukawa matrices will not be quantitatively affected by the addition of this extra dimension.

We now briefly summarize the gauge unification results given by Kim and Raby [20]. A 5D gauge theory is nonrenormalizable and gets large corrections at the cutoff.

Corrections to gauge couplings, however, will be the same for all couplings unified into the larger gauge group. These corrections will affect the absolute values of the gauge couplings, but not the differences. Further, if the gauge symmetry is broken only by orbifolding or by Higgs mechanism on the branes, the differences in the couplings will have a logarithmic, calculable running.

The states which affect the differential running are the bulk vector multiplet \mathcal{V} and the bulk Higgs hypermultiplet \mathcal{H} .⁴ The placement and number of complete matter multiplets does not affect gauge coupling unification, since matter multiplets (16s of SO(10)) act equally across the three gauge couplings and cannot affect the coupling differences. Those states in the theory outside of the MSSM have twisted orbifold boundary conditions and so have masses at the compactification scale (M_c). For energies below M_c , the theory is the MSSM. The effects of running between M_c and M_* (the cutoff scale), including the Kaluza-Klein (KK) towers, are taken as threshold corrections at M_c . Without these threshold corrections, it is known that the MSSM unifies around $M_G \sim 3 \times 10^{16}$ GeV with a coupling of $\alpha_{\text{GUT}} \sim 1/24$ and a GUT-scale threshold correction for α_3 of $\varepsilon_3 \sim -0.04$. Assuming unification in the orbifold theory at the cutoff scale M_* and that the PS breaking Higgs VEV is of order the cutoff scale, we can solve for M_* and M_c in terms of the 4D GUT parameters M_G , α_{GUT} , and ε_3 . This leads to $M_* \sim 10^{17}$ GeV and $M_c \sim 10^{14}$ GeV [20].

The matter field locations are constrained by proton decay:

- Matter fields on the SO(10) brane

There are gauge bosons within SO(10) which mediate baryon (B) and lepton (L) number-violating interactions. All of these are outside of the Standard Model and hence have masses of order M_c or higher. After integrating out these fields (and their KK modes), we get dimension six operators which violate B and L for any matter multiplets on the SO(10) brane. These operators are suppressed by $1/M_c^2$. Given $M_c \sim 10^{14}$ GeV, current bounds on proton decay rule out models which have these operators for the first and second families. Thus only the third family can reside on the SO(10) brane [44].⁵ Dimension 5 proton decay operators

⁴When considering differential running of the gauge couplings, a Higgs hypermultiplet in the bulk is effectively the same as a 4D 10 of SO(10) with light Higgs MSSM doublets and heavy Higgs triplets of mass M_c . This setup admits gauge coupling unification as shown by Kim and Raby [20]. In particular, see the calculations leading to equation (3.13) of that paper. Effects from brane Higgs doublets would be felt up to M_* and would tend to inhibit unification since they drive the couplings apart rather than together.

⁵With dimension six operators for the third family, mixing between this family and the first two can induce proton decay. Assuming that the mixing is of order $|V_{ub}|$ or $|V_{cb}|$ and that the gauge bosons have

vanish since the color triplet Higgs states obtain off-diagonal mass with triplets in $\overline{10}$ and these states do not couple to matter.

- Matter fields on the PS brane or in the bulk

Pati-Salam gauge symmetry does not relate the left-handed fields ψ ($(4, 2, 1)$ in PS) to the right-handed fields ψ^c ($(\overline{4}, 1, 2)$ in PS), and we do not get baryon number-violating dimension six operators after integrating out the heavy gauge bosons. Therefore, any matter fields can be on the PS brane as long as the PS breaking scale is not extremely low. This scale in our theory is $M_* \sim 10^{17}$ GeV, and proton decay is not a problem here.

In principle, we can consider higher dimensional operators with derivative interactions $\partial_5 = \partial/\partial y$. Because the coefficients of the higher dimensional operators are not determined from the theory we cannot calculate the proton decay rate from these operators accurately. However, we can get a bound that is consistent with our setup by assuming unknown coefficients to be order one. See Kim and Raby for more details [20].

Proton decay constrains the first and second families to reside either in the bulk or on the PS brane, but does not constrain the location of the third family. We choose to place the third family on the SO(10) brane. Given this placement, the second family is forced to reside on the PS brane. If it were in the bulk, volume suppression would give $m_\mu/m_\tau \sim 10^{-3}$, which is far too small to fit the data. Our D_3 flavor symmetry places the first and second families together into a doublet, so we place both on the PS brane.

Let us summarize the basic setup.

- Gauge symmetry : SO(10) in the bulk and at $y = 0$, Pati-Salam at $y = \pi R/2$.
- Higgs fields come from 10 dimensional hypermultiplets in the bulk.
- 3rd family matter fields are on the SO(10) brane.
- 1st and 2nd family matter fields, a doublet under D_3 , are on the PS brane.
- Kink mass localizes the hypermultiplets through their X -dependence.

mass at M_c , naive calculations using formulae in [44] put the proton lifetime many orders of magnitude above current limits, since this leads to an effective gauge boson mass of order $M_c/(V_{cb}V_{ub}) \approx 6 \times 10^{17}$ GeV.

Table 1: Bulk fields

Field	PS Symm	D ₃ Symm
$16 = \begin{pmatrix} \psi_{--} \\ \psi_{-+}^c \end{pmatrix}$	$\begin{pmatrix} (4, 2, 1) \\ (\bar{4}, 1, 2) \end{pmatrix}$	$\mathbf{2}_A$
$\bar{16} = \begin{pmatrix} \bar{\psi}_{++} \\ \psi_{+-}^c \end{pmatrix}$	$\begin{pmatrix} (\bar{4}, 2, 1) \\ (4, 1, 2) \end{pmatrix}$	$\mathbf{2}_A$
$10 = \begin{pmatrix} H_{++} \\ H_{+-}^c \end{pmatrix}$	$\begin{pmatrix} (1, 2, 2) \\ (6, 1, 1) \end{pmatrix}$	$\mathbf{1}_A$
$\bar{10} = \begin{pmatrix} \bar{H}_{--} \\ \bar{H}_{-+}^c \end{pmatrix}$	$\begin{pmatrix} (1, 2, 2) \\ (6, 1, 1) \end{pmatrix}$	$\mathbf{1}_A$

3.2 Yukawa Matrix

This section introduces the fields and superpotential of our model. Here we calculate the Yukawa matrices associated with the massless fields corresponding to the Standard Model fermions.

First we introduce the matter content of the theory. In the bulk, we have two 5D N=1 hypermultiplets which transform as 16s under SO(10). These fields form a doublet ($\mathbf{2}_A$) under the D₃ family symmetry. In our Lagrangian, we show the D₃ doublet structure of these fields by a subscript a , with $a = 1, 2$. For information on how doublets and other D₃ objects couple, please see Appendix A. We also have a hypermultiplet 10 of SO(10) which is a singlet ($\mathbf{1}_A$) under the family symmetry. These fields are listed in Table 1 with their parities, PS gauge symmetries, and family symmetries. On the SO(10) brane we place a single 16 of SO(10), invariant under D₃, and an SO(10) gauge singlet ϕ which is a doublet under the family symmetry. These fields are listed in Table 2. The PS brane has a more complicated set of fields. There are the fields ψ and ψ^c , each doublets under D₃, which transform as the two halves of an SO(10) 16. N^c and \bar{N}^c are also family doublets and carry charge under PS in order to allow mixing between ψ^c and N^c . There are various other fields $\tilde{\phi}$, A , A_{3R} , ω^c , and $\bar{\omega}^c$ which will get vacuum expectation values. These fields are listed in Table 3 with their PS charges and D₃ family symmetries.

We choose to break the superpotential into two pieces: $W = W_1 + W_2$. The first contains terms leading to interactions between the matter and Higgs field ($H \equiv H_{++}$):

$$\begin{aligned}
 W_1 = & \left[\frac{1}{2} \lambda_3 16_3 10 16_3 \right] \delta(y) \\
 & + \left[\lambda_\alpha \psi_a H \psi_a^c A + \lambda_\beta \psi_a H N_a^c \tilde{\phi}_a + 2\lambda_\gamma \psi_a H A_{3R} (\psi_{-+}^c)_a \right] \delta(y - \frac{\pi R}{2})
 \end{aligned}
 \tag{3.11}$$

Table 2: SO(10) Brane fields

Field	PS Symm	D ₃ Symm
$16_3 = \begin{pmatrix} \psi_3 \\ \psi_3^c \end{pmatrix}$	$\begin{pmatrix} (4, 2, 1) \\ (\bar{4}, 1, 2) \end{pmatrix}$	$\mathbf{1}_A$
ϕ	$(1, 1, 1)$	$\mathbf{2}_A$

Table 3: PS Brane fields

Field	PS Symm	D ₃ Symm
ψ	$(4, 2, 1)$	$\mathbf{2}_A$
ψ^c	$(\bar{4}, 1, 2)$	$\mathbf{2}_A$
N^c	$(\bar{4}, 1, 2)$	$\mathbf{2}_A$
$\overline{N^c}$	$(4, 1, 2)$	$\mathbf{2}_A$
$\tilde{\phi}$	$(1, 1, 1)$	$\mathbf{2}_A$
A	$(1, 1, 1)$	$\mathbf{1}_B$
A_{3R}	$(1, 1, 3)$	$\mathbf{1}_A$
ω^c	$(\bar{4}, 1, 2)$	$\mathbf{1}_A$
$\overline{\omega^c}$	$(4, 1, 2)$	$\mathbf{1}_A$

W_2 contains mass terms:

$$\begin{aligned}
W_2 = & \overline{16}_a(\partial_y - m_X)16_a + \overline{10}(\partial_y - m_X)10 \\
& + [2\sigma\phi_a\overline{16}_a16_3] \delta(y) \\
& + [2\eta(\overline{\psi}_{++})_a\chi_a + \overline{N^c}_a(a\psi_a^c + b_0\omega^c\overline{\omega^c}N_a^c)] \delta(y - \frac{\pi R}{2})
\end{aligned} \tag{3.12}$$

Sufficient factors of the cutoff scale M_* should be placed in the superpotential terms so that the couplings λ_3 , λ_α , λ_β , λ_γ , σ , η , a , and b_0 are dimensionless. We assume that at this stage our Lagrangian possesses a CP-symmetry and that these couplings are all real. All CP-violation will come from spontaneous symmetry breaking. The fields which get VEVs are ϕ_1 , ϕ_2 , $\tilde{\phi}_2$, A , A_{3R} , ω^c , and $\overline{\omega^c}$. The first 4 break D₃ symmetry, while $\langle A_{3R} \rangle = A_{3R}^0 T_{3R}$ breaks SU(2)_R symmetry. All of these VEVs we take to be real. ω^c and $\overline{\omega^c}$ are fields which get VEVs in the right-handed neutrino direction. These VEVs we take to be complex, and furthermore take the combination to be in a particular direction: $\langle \omega^c \overline{\omega^c} \rangle \propto ce^{i\theta_1} + X_R e^{i\theta_2}$. More will be said later about this choice of direction. All of the above mentioned VEV values are taken to be of order M_* rather than M_c , but are allowed to lie enough below M_* to be able to give the desired

hierarchies in the Yukawa matrices. We also assume that the fields listed here, which get VEVs, obtain mass near the cutoff scale M_* . This lifts these fields high enough that they cannot adversely affect the gauge coupling unification results we wish to preserve.

Our superpotential allows 9 extra U(1) symmetries which we take to be symmetries of the theory in order to forbid problematic superpotential terms.⁶ We choose to parametrize these symmetries by the following 9 fields: H_{+-}^c , ψ_3 , ψ_3^c , ψ_a , A , A_{3R} , ω^c , and $\overline{\omega^c}$. We choose each of these fields to have an arbitrary charge under one and only one U(1). After specifying these charges, the charges of the remaining fields are determined by the terms in the superpotential. In addition to these U(1)s, the superpotential can have Z_2 symmetries which are extensions of the first orbifold Z_2 . The transformations of the bulk fields under this symmetry have already been given. To have such a symmetry, we can choose A_{3R} odd and the remaining 7 independent fields (H_{+-}^c is already determined) even under this Z_2 . The transformations of the remaining fields can then be determined from the superpotential terms. Another possible choice is ψ_a odd with the remaining fields even. It can be shown that it is not possible to similarly extend the second Z_2 orbifold to the brane terms of the superpotential.

Our 5D bulk Higgs field $H(x^\mu, y)$ can be represented as a 4D massless state and a KK tower of 4D massive states. In order to find the effective Yukawa matrices, we need to know the overlap between the 5D bulk field $H(x^\mu, y)$ and the effective 4D massless Higgs $H^0(x^\mu)$.⁷ This overlap is

$$H(x^\mu, y) \supset e^{\frac{X_H \zeta y}{\pi R}} n_H \rho \sqrt{M_*} H^0(x^\mu) \quad (3.13)$$

where

$$n_X \equiv \sqrt{\frac{X\zeta}{e^{X\zeta} - 1}} \quad (3.14)$$

$$\rho \equiv \sqrt{\frac{2M_c}{\pi M_*}}.$$

The kink mass dependence gives the massless Higgs field an exponential profile, localizing it to an end of the extra dimension. We will use n_X , n_H , n_L , n_R , etc. to stand for a normalization as above with the particular value for the X quantum number substituted for the X in equation (3.14). In the same manner, at times we will use n_1 or

⁶We can avoid unwanted flavor changing neutral currents from the breaking of these extra symmetries by instead assuming only Z_n subgroups of the U(1)s sufficient to forbid the unwanted superpotential terms.

⁷When addressing the overlap between 5D and 4D fields, to avoid confusion we will explicitly show the dependence of the fields on the spacetime coordinates.

n_{-3} to refer to these normalization factors with the indicated X value inserted. We can see explicitly in equation (3.13) that the up- and down-Higgs wavefunctions are localized towards opposite ends of the y direction domain $[0, \frac{\pi R}{2}]$ due to their opposite X quantum numbers.

The light fields which will correspond to our observed three families of particles come from various mixings of the fields in the superpotential. Consider the following terms contained in W_2 :

$$W_2 \supset [\overline{N}_a^c (a\psi_a^c + b_0\omega^c\overline{\omega}^c N_a^c)] \delta(y - \frac{\pi R}{2}) \quad (3.15)$$

With the factors of M_* explicit:

$$b_0 \left(\frac{\omega^c\overline{\omega}^c}{M_*^2} \right) \xrightarrow{\text{VEV}} b'_0 (ce^{i\theta_1} + X_R e^{i\theta_2}) \equiv b \quad (3.16)$$

One combination of ψ_a^c and N_a^c is massive while the other combination leads to a massless field. In terms of a and b , the overlap between the massless field ψ_a^{c0} and the original fields is:

$$\begin{aligned} \psi_a^c &\supset n^c \psi_a^{c0} \\ N_a^c &\supset -\frac{a}{b} n^c \psi_a^{c0} \\ n^c &\equiv \frac{1}{\sqrt{1 + \frac{a^2}{|b|^2}}} \end{aligned} \quad (3.17)$$

The light fields ψ_a^{c0} form a D_3 doublet and correspond to the 1st and 2nd family right-handed particles. The factor of $\frac{a}{b}$ in the overlap between N_a^c and ψ_a^{c0} will lead to $\frac{1}{b} \propto \frac{1}{ce^{i\theta_1} + X_R e^{i\theta_2}}$ in the (2,2) elements of the Yukawa matrices. This factor is important in fitting inter-family fermion mass ratios and in providing us with nontrivial phases in the Yukawa matrices.

Now we turn to a different subset of W_2 :

$$\begin{aligned} W_2 &\supset \overline{16}_a (\partial_y - m_X) 16_a \\ &+ [2\sigma\phi_a \overline{16}_a 16_3] \delta(y) + [2\eta (\overline{\psi}_{++})_a \chi_a] \delta(y - \frac{\pi R}{2}) \end{aligned} \quad (3.18)$$

These mass terms lead to mixing between the brane fields $16_3(x^\mu)$, $\chi_a(x^\mu)$ and the bulk fields $16_a(x^\mu, y)$. The overlap between the resulting left-handed massless field ($\psi_3^0(x^\mu)$) and those fields in the superpotential:

$$\psi_3(x^\mu) \supset \tilde{n}_L \psi_3^0(x^\mu) \quad (3.19)$$

$$\begin{aligned}
(\psi_{--})_a(x^\mu, y) &\supset -\varepsilon_{--}(y) e^{\frac{X_L \zeta y}{\pi R}} \left(\frac{\phi_a}{M_*} \right) \sigma \sqrt{M_*} \tilde{n}_L \psi_3^0(x^\mu) \\
\chi_a(x^\mu) &\supset -e^{\frac{X_L \zeta}{2}} \left(\frac{\phi_a}{M_*} \right) \frac{\sigma}{\eta} \tilde{n}_L \psi_3^0(x^\mu)
\end{aligned}$$

The overlap in the right-handed fields is

$$\begin{aligned}
\psi_3^c(x^\mu) &\supset \tilde{n}_R \psi_3^{c0}(x^\mu) \\
(\psi_{-+})_a(x^\mu, y) &\supset -\varepsilon_{-+}(y) e^{\frac{X_R \zeta y}{\pi R}} \left(\frac{\phi_a}{M_*} \right) \sigma \sqrt{M_*} \tilde{n}_R \psi_3^{c0}(x^\mu).
\end{aligned} \tag{3.20}$$

The definitions of $\varepsilon_{-+}(y)$ and $\varepsilon_{--}(y)$ have been given in equation (3.7). ψ_3^0 and ψ_3^{c0} correspond to the left- and right-handed 3rd family fields. Other definitions follow:

$$\begin{aligned}
\tilde{n}_L &\equiv \frac{1}{\sqrt{1 + r^2 \left[\frac{1}{n_L^2} + \frac{\rho^2}{\eta^2} e^{X_L \zeta} \right]}} \\
\tilde{n}_R &\equiv \frac{1}{\sqrt{1 + r^2 \frac{1}{n_R^2}}} \\
r^2 &\equiv \frac{\sigma^2}{\rho^2} \left[\left(\frac{\phi_1}{M_*} \right)^2 + \left(\frac{\phi_2}{M_*} \right)^2 \right]
\end{aligned} \tag{3.21}$$

For more information on our treatment of these overlaps and normalizations, please see Appendix B.

The left-handed 1st and 2nd family fields are equal to ψ_a , which do not mix with any other fields. We replace all fields within W_1 with their massless components. This yields the X -dependent Yukawa matrices for the massless fields with left-handed doublets on the left:

$$Y = \begin{pmatrix} 0 & \alpha_0 \frac{n^c}{LR} & \varepsilon_0 \frac{2T_{3R}}{L} \\ -\alpha_0 \frac{n^c}{LR} & \beta_0 \frac{b_0^c n^c}{b LR} & \gamma_0 \frac{2T_{3R}}{L} \\ 0 & 0 & 1 \end{pmatrix} \lambda. \tag{3.22}$$

Definitions follow:⁸

$$\begin{aligned}
L &\equiv e^{\frac{X_L \zeta}{2}} \tilde{n}_L \\
R &\equiv e^{\frac{X_R \zeta}{2}} \tilde{n}_R \\
\lambda &\equiv \lambda_3 \rho \tilde{n}_L \tilde{n}_R n_H
\end{aligned} \tag{3.23}$$

⁸We use the fact that for all Yukawa terms, $X_L + X_R + X_H = 0$.

$$\begin{aligned}
\alpha_0 &\equiv \frac{\lambda_\alpha \langle A \rangle}{\lambda_3 M_*} \\
\beta_0 &\equiv -\frac{\lambda_\beta \langle \tilde{\phi}_2 \rangle a}{\lambda_3 M_* b'_0} \\
\gamma_0 &\equiv -\frac{\lambda_\gamma A_{3R}^0 \langle \phi_1 \rangle}{\lambda_3 M_* M_*} \sigma \\
\varepsilon_0 &\equiv \gamma_0 \frac{\phi_2}{\phi_1}
\end{aligned}$$

The Yukawa matrices may be simplified by looking at the normalization constant n^c . We assume that $a \ll |b|$, and so we can approximate $n^c \sim 1$. This is not incompatible with our definition of β_0 , as we also expect $\beta_0 \ll 1$.

An approximation may also be made within \tilde{n}_L .

$$\begin{aligned}
\tilde{n}_L &\equiv \frac{1}{\sqrt{1 + r^2 \left[\frac{1}{n_L^2} + \frac{\rho^2}{\eta^2} e^{X_L \zeta} \right]}} \\
&\simeq \frac{1}{\sqrt{1 + r^2 \frac{1}{n_L^2}}}
\end{aligned} \tag{3.24}$$

We assume that $\eta \gtrsim \mathcal{O}(1)$, and since $\rho \sim 1/40$ for reasonable values of the compactification and cutoff scales derived from gauge coupling unification, $\frac{\rho^2}{\eta^2} e^{X_L \zeta} \ll \frac{1}{n_L^2}$ for $-10 < \zeta < 10$, which easily encompasses the ζ -range which has a chance of fitting the data.

It is convenient to reparametrize r^2 in terms of other variables. With the definition

$$\kappa \equiv \left(\frac{\lambda_3 M_*}{\lambda_\gamma A_{3R}^0} \right) \tag{3.25}$$

r^2 may be rewritten as

$$r^2 = \frac{\kappa^2}{\rho^2} (\gamma_0^2 + \varepsilon_0^2). \tag{3.26}$$

With this redefinition the normalization constants \tilde{n}_L and \tilde{n}_R become

$$\tilde{n}_X = \frac{1}{\sqrt{1 + \frac{\kappa^2}{\rho^2} \frac{\gamma_0^2 + \varepsilon_0^2}{n_X^2}}} \tag{3.27}$$

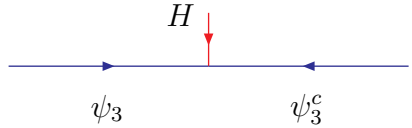
It is this definition for the \tilde{n}_X which we will use throughout the rest of this paper.

Under the approximation of $n^c \sim 1$, the Yukawa matrices simplify to:

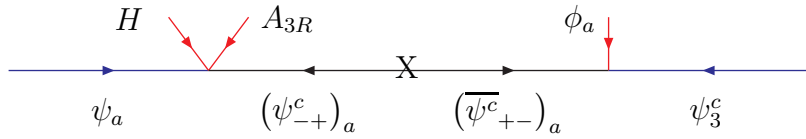
$$Y = \begin{pmatrix} 0 & \alpha_0 \frac{1}{LR} & \varepsilon_0 \frac{2T_{3R}}{L} \\ -\alpha_0 \frac{1}{LR} & \beta_0 \frac{b'_0}{b} \frac{1}{LR} & \gamma_0 \frac{2T_{3R}}{L} \\ 0 & 0 & 1 \end{pmatrix} \lambda. \quad (3.28)$$

These are the Yukawa matrices which we will analyze in the next section.⁹

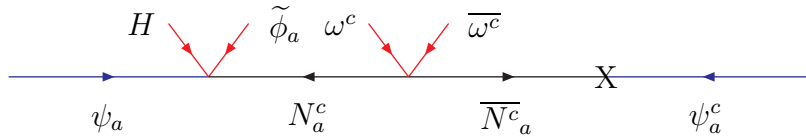
The lowest order diagrams which contribute to the Yukawa matrices follow. For each diagram we give the Yukawa element(s) to which it contributes.



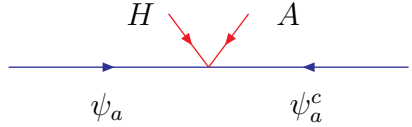
$$(3,3)$$



$$(1,3) (2,3)$$



$$(2,2)$$



$$(1,2) (2,1)$$

4. Analysis

We take two routes in the analysis of our model. In the first subsection we use analytic methods to extract predictions from our theory. Relations between the Yukawa parameters and the observables are given but are not solved due to the complexity of the equations. A more precise numerical analysis, in which a full fit is achieved, is then given in the following subsection.

⁹We could have included terms in our superpotential allowing (3,1) and (3,2) elements in the Yukawa matrices. However, as long as such matrix elements are hierarchical, they cannot affect the theoretical values of the low energy observables. Such terms are also not necessary in our theory (e.g., we do not have a left-right symmetry which requires their presence) and so we have left them out of our superpotential.

4.1 Analytic Fitting

The starting point for our analysis is the Yukawa matrix of equation (3.28). In our model, this Yukawa matrix is defined at the compactification scale M_c . We have taken into account the effects of integrating out the heavy fields but have neglected the running effects on the Yukawa matrix elements between M_* (where the superpotential of equations (3.11) and (3.12) is defined) and M_c . We assume that these running effects are small enough to ignore at the level of a few percent.

To make the analysis easier, we define α_u, α_d , etc. below.

$$\begin{aligned}
Y(X) &= \begin{pmatrix} 0 & \alpha_0 \frac{e^{X_H \zeta/2}}{\tilde{n}_L \tilde{n}_R} & \varepsilon_0 2T_{3R} \frac{e^{-X_L \zeta/2}}{\tilde{n}_L} \\ -\alpha_0 \frac{e^{X_H \zeta/2}}{\tilde{n}_L \tilde{n}_R} & \frac{\beta_0}{ce^{i\theta_1} + X_R e^{i\theta_2}} \frac{e^{X_H \zeta/2}}{\tilde{n}_L \tilde{n}_R} & \gamma_0 2T_{3R} \frac{e^{-X_L \zeta/2}}{\tilde{n}_L} \\ 0 & 0 & 1 \end{pmatrix} \lambda_x \quad (4.1) \\
&\equiv \begin{pmatrix} 0 & \alpha_x & \varepsilon_x \\ -\alpha_x & \beta_x & \gamma_x \\ 0 & 0 & 1 \end{pmatrix} \lambda_x
\end{aligned}$$

After inputting the proper X quantum numbers:

$$\begin{aligned}
\alpha_u &\equiv \alpha_0 e^{-\zeta} \frac{1}{(\tilde{n}_1)^2} & \alpha_d &\equiv \alpha_0 e^\zeta \frac{1}{\tilde{n}_1 \tilde{n}_{-3}} & \alpha_e &\equiv \alpha_0 e^\zeta \frac{1}{\tilde{n}_1 \tilde{n}_{-3}} \\
\beta_u &\equiv \frac{1}{ce^{i\theta_1} + e^{i\theta_2}} \beta_0 e^{-\zeta} \frac{1}{(\tilde{n}_1)^2} & \beta_d &\equiv \frac{1}{ce^{i\theta_1} - 3e^{i\theta_2}} \beta_0 e^\zeta \frac{1}{\tilde{n}_1 \tilde{n}_{-3}} & \beta_e &\equiv \frac{1}{ce^{i\theta_1} + e^{i\theta_2}} \beta_0 e^\zeta \frac{1}{\tilde{n}_1 \tilde{n}_{-3}} \\
\gamma_u &\equiv -\gamma_0 e^{-\zeta/2} \frac{1}{\tilde{n}_1} & \gamma_d &\equiv \gamma_0 e^{-\zeta/2} \frac{1}{\tilde{n}_1} & \gamma_e &\equiv \gamma_0 e^{3\zeta/2} \frac{1}{\tilde{n}_{-3}} \\
\varepsilon_u &\equiv -\varepsilon_0 e^{-\zeta/2} \frac{1}{\tilde{n}_1} & \varepsilon_d &\equiv \varepsilon_0 e^{-\zeta/2} \frac{1}{\tilde{n}_1} & \varepsilon_e &\equiv \varepsilon_0 e^{3\zeta/2} \frac{1}{\tilde{n}_{-3}} \\
\lambda_t & & \lambda_b &= \lambda_t e^{-\zeta} \frac{\tilde{n}_{-3}}{\tilde{n}_1} & \lambda_\tau &= \lambda_t e^{-\zeta} \frac{\tilde{n}_{-3}}{\tilde{n}_1}
\end{aligned} \quad (4.2)$$

and

$$\tilde{n}_X = \frac{1}{\sqrt{1 + \frac{\kappa^2 \gamma_0^2 + \varepsilon_0^2}{\rho^2 n_X^2}}} \quad (4.3)$$

There are eleven parameters associated with the fermion masses derived from the Yukawa matrices: $\zeta, \alpha_0, \beta_0, \gamma_0, \varepsilon_0, c, \theta_1, \theta_2, \kappa, \lambda_t$, and $\tan \beta$. Because there are 13 independent observables in the quark and charged lepton sectors: 9 masses, 3 quark mixing angles, and the CP-violating phase in the CKM matrix, we can expect two predictions in this model.

We assume that both of the quark Yukawa matrices are hierarchical [45]. As we explained within [46] this allows us to use a simple set of rotations to diagonalize our

quark mass matrices and leads to a simple CKM matrix:

$$V_{CKM} = \begin{pmatrix} 1 & s_{12}^* + s_{13}^{U*} s_{23} & -s_{12}^{U*} s_{23}^* + s_{13}^* \\ -s_{12} - s_{13}^D s_{23}^* & 1 & s_{23}^* + s_{12}^U s_{13}^* \\ s_{12}^D s_{23} - s_{13} & -s_{23} - s_{12}^{D*} s_{13} & 1 \end{pmatrix}, \quad (4.4)$$

where

$$\begin{aligned} s_{12}^U &\simeq \frac{\alpha_u}{\beta_u}, & s_{12}^D &\simeq \frac{\alpha_d}{\beta_d}, & s_{12} &\equiv s_{12}^D - s_{12}^U, \\ s_{13}^U &\simeq \varepsilon_u, & s_{13}^D &\simeq \varepsilon_d, & s_{13} &\equiv s_{13}^D - s_{13}^U, \\ s_{23}^U &\simeq \gamma_u, & s_{23}^D &\simeq \gamma_d, & s_{23} &\equiv s_{23}^D - s_{23}^U. \end{aligned} \quad (4.5)$$

The eigenvalues of the diagonalized quark Yukawa matrices lead to the quark masses:

$$\begin{aligned} m_t &\simeq \lambda_t \frac{v_u}{\sqrt{2}} & \frac{m_c}{m_t} &\simeq |\beta_u| & \frac{m_u}{m_c} &\simeq \frac{\alpha_u^2}{|\beta_u|^2} \\ m_b &\simeq \lambda_b \frac{v_d}{\sqrt{2}} & \frac{m_s}{m_b} &\simeq |\beta_d| & \frac{m_d}{m_s} &\simeq \frac{\alpha_d^2}{|\beta_d|^2} \end{aligned} \quad (4.6)$$

We will take the charged lepton Yukawa matrix to be lopsided to some extent, with $\gamma_e \sim \mathcal{O}(1)$ and the rest of the matrix following a hierarchy.¹⁰ This choice leads to the charged lepton masses:

$$m_\tau \simeq \lambda_\tau \frac{v_d}{\sqrt{2}} \sqrt{1 + \gamma_e^2} \quad \frac{m_\mu}{m_\tau} \simeq \frac{|\beta_e|}{1 + \gamma_e^2} \quad \frac{m_e}{m_\mu} \simeq \frac{\alpha_e^2}{|\beta_e|^2} \sqrt{1 + \gamma_e^2} \quad (4.7)$$

We want to use the kink mass, here parametrized by ζ , to localize the two Higgs wave functions to opposite branes. As stated before, if H_u is localized towards the SO(10) brane and H_d is localized towards the PS brane, then there is a natural reason why m_t is larger than m_b while m_u is smaller than m_d . As can be seen from the α_x (equation (4.2)), which play a large part in determining the masses of the first family fermions, if $\zeta > 0$ we have m_u suppressed by $e^{-\zeta}$ and m_d enhanced by e^ζ . Similarly, the third family masses have the opposite dependence as shown in the relation: $\lambda_b = \lambda_t e^{-\zeta \frac{\tilde{n}-3}{\tilde{n}_1}}$. Looking at γ_x , we see that $\zeta > 0$ enhances γ_e while suppressing γ_u and γ_d , so it is not unreasonable to assume that $\gamma_e \sim 1$ while $\gamma_u, \gamma_d \ll 1$.

With a few approximations within the CKM matrix the mixing angles and CP-violating angle β are:

$$|V_{us}| \simeq |s_{12}^* + s_{13}^{U*} s_{23}| \simeq |s_{12}| \simeq \left| \frac{\alpha_d}{\beta_d} \right| \left| 1 - \frac{\alpha_u \beta_d}{\beta_u \alpha_u} \right| \quad (4.8)$$

$$|V_{cb}| \simeq |s_{23}^* + s_{12}^U s_{13}^*| \simeq |s_{23}| \simeq |\gamma_d - \gamma_u|$$

¹⁰The lopsided effect with order one γ_e is crucial to achieve correct b- τ unification [47].

$$|V_{ub}| \simeq |s_{13}^* - s_{12}^U s_{23}^*| \simeq |\varepsilon_d - \varepsilon_u| \left| 1 - \frac{\alpha_u (\gamma_d - \gamma_u)}{\beta_u (\varepsilon_d - \varepsilon_u)} \right|$$

$$\beta \equiv \arg \left(-\frac{V_{cd} V_{cb}^*}{V_{td} V_{tb}^*} \right) \simeq \arg \left(1 - \frac{\alpha_u \beta_d}{\beta_u \alpha_d} \right) - \arg \left(1 - \frac{\beta_d (\varepsilon_d - \varepsilon_u)}{\alpha_d (\gamma_d - \gamma_u)} \right)$$

With hierarchical structure in the up and down quark matrices it is the case that $|V_{cb}| \sim \left| \frac{(2,3)_D}{(3,3)_D} - \frac{(2,3)_U}{(3,3)_U} \right|$. Here this is reflected in the relation $|V_{cb}| \simeq |\gamma_d - \gamma_u|$. To have a nonzero V_{cb} , we need to have some dependence on right-handed quantum numbers within γ_x . We have found that in our setup, regardless of the placement of fields, the kink mass effects (which come with ζX) can only bring X_L into the Yukawa element ratio $\frac{(2,3)}{(3,3)}$. For this reason we have added the field A_{3R} to the superpotential, and it is the VEV of this field (proportional to T_{3R}) which gives us the necessary difference between γ_d and γ_u to generate a nonzero V_{cb} .

The structure of the (2, 2) Yukawa elements, proportional to $\frac{1}{ce^{i\theta_1} + X_R e^{i\theta_2}}$, helps us to fit several observables. The X_R dependence gives different phases between the up and down elements, both of which contribute to the CKM matrix CP-violating phase β . The phase of β_u is also important in fitting the size of $|V_{ub}|$. In addition, the magnitude of these (2, 2) elements helps us to fit the first to second and second to third family mass ratios.

We will now show the predictions of this model in the form of relations between observables at the compactification scale. Consider the fermion mass combinations $\left(\frac{m_\tau}{m_b}\right)$ and $\left(\frac{m_u}{m_c}\right) / \left(\frac{m_e}{m_\mu}\right)$:

$$\left(\frac{m_\tau}{m_b}\right) (M_c) \simeq \frac{\lambda_\tau}{\lambda_b} \sqrt{1 + \gamma_e^2} = \sqrt{1 + \gamma_e^2} \quad (4.9)$$

$$\left(\frac{m_u}{m_c}\right) / \left(\frac{m_e}{m_\mu}\right) (M_c) \simeq \frac{\alpha_u^2 |\beta_e|^2}{\alpha_e^2 |\beta_u|^2} \frac{1}{\sqrt{1 + \gamma_e^2}} = \frac{1}{\sqrt{1 + \gamma_e^2}}$$

One prediction of this model is then

$$\left(\frac{m_u}{m_c}\right) / \left(\frac{m_e}{m_\mu}\right) (M_c) \simeq \left(\frac{m_b}{m_\tau}\right) (M_c). \quad (4.10)$$

Consider also the determinants of the down quark and charged lepton mass matrices.

$$m_d m_s m_b (M_c) = |\det Y_d| \left(\frac{v_d}{\sqrt{2}}\right)^3 = \alpha_d^2 \lambda_b \left(\frac{v_d}{\sqrt{2}}\right)^3 \quad (4.11)$$

$$m_e m_\mu m_\tau (M_c) = |\det Y_e| \left(\frac{v_d}{\sqrt{2}}\right)^3 = \alpha_e^2 \lambda_\tau \left(\frac{v_d}{\sqrt{2}}\right)^3$$

Because $\alpha_d = \alpha_e$ and $\lambda_b = \lambda_\tau$, we have the (exact) prediction:

$$m_d m_s m_b(M_c) = m_e m_\mu m_\tau(M_c) \quad (4.12)$$

These two predictions hold regardless of the actual values taken on by the Yukawa parameters.

As for the Yukawa parameter values themselves, these must be determined from the eleven remaining independent observables, if possible. The dependence of these observables on the parameters is complicated enough that we find it impossible to make a fit nonnumerically. Actual fit values for the Yukawa parameters must wait until the numerical analysis in Section 4.2.

Our predictions are relations at the compactification scale, while our data has been taken at the weak scale. In order to determine the extent to which our predictions are reasonable, we need to estimate the renormalization effects on the masses between the two scales. In this analysis, we choose to diagonalize the Yukawa matrices at the compactification scale, and use the RG formalism of Barger, Berger, and Ohmann [48] to relate the observables at M_Z (or at m_t in the case of the top quark) to their values at M_c with simple scaling relations.

$$M_u^{\text{diag}}(M_c) = \begin{pmatrix} S_u(M_Z, M_c)m_u(M_Z) & 0 & 0 \\ 0 & S_u(M_Z, M_c)m_c(M_Z) & 0 \\ 0 & 0 & S_t(m_t, M_c)m_t(m_t) \end{pmatrix} \quad (4.13)$$

$$M_d^{\text{diag}}(M_c) = \begin{pmatrix} S_d(M_Z, M_c)m_d(M_Z) & 0 & 0 \\ 0 & S_d(M_Z, M_c)m_s(M_Z) & 0 \\ 0 & 0 & S_b(M_Z, M_c)m_b(M_Z) \end{pmatrix}$$

$$M_e^{\text{diag}}(M_c) = \begin{pmatrix} S_e(M_Z, M_c)m_e(M_Z) & 0 & 0 \\ 0 & S_e(M_Z, M_c)m_\mu(M_Z) & 0 \\ 0 & 0 & S_\tau(M_Z, M_c)m_\tau(M_Z) \end{pmatrix}$$

$$|V|^2(M_c) = \begin{pmatrix} |V_{ud}|^2(M_Z) & |V_{us}|^2(M_Z) & S(M_Z, M_c)|V_{ub}|^2(M_Z) \\ |V_{cd}|^2(M_Z) & |V_{cs}|^2(M_Z) & S(M_Z, M_c)|V_{cb}|^2(M_Z) \\ S(M_Z, M_c)|V_{td}|^2(M_Z) & S(M_Z, M_c)|V_{ts}|^2(M_Z) & |V_{tb}|^2(M_Z) \end{pmatrix}$$

The scaling factors S can be found in [48]. In deriving these scaling factors, the authors have used 2-loop running and have included running effects from the gauge couplings and the third family Yukawa couplings. We make a further approximation in that we keep only 1-loop effects and neglect all running effects from the Yukawa sector except for the top Yukawa coupling. With these approximations

$$\begin{aligned}
S_u(M_Z, M_c) &\simeq y_t^{-3}(m_t, M_c)G_u(M_Z, M_c) \\
S_t(m_t, M_c) &\simeq y_t^{-6}(m_t, M_c)G_u(m_t, M_c) \\
S_d(M_Z, M_c) &\simeq G_d(M_Z, M_c) \\
S_b(M_Z, M_c) &\simeq y_t^{-1}(m_t, M_c)G_d(M_Z, M_c) \\
S_e(M_Z, M_c) &\simeq G_e(M_Z, M_c) \\
S_\tau(M_Z, M_c) &\simeq G_e(M_Z, M_c) \\
S(M_Z, M_c) &\simeq y_t^2(m_t, M_c)
\end{aligned} \tag{4.14}$$

with

$$y_t(m_t, M_c) \equiv \exp \left[-\frac{1}{16\pi^2} \int_{m_t}^{M_c} \lambda_t^2(\mu) d(\log \mu) \right] \tag{4.15}$$

$$\begin{aligned}
G_x(M_Z, M_c) &\equiv \exp \left[-\frac{1}{16\pi^2} \int_{M_Z}^{M_c} \sum_i c_i^x g_i^2(\mu) d(\log \mu) \right] \\
&= \prod_i \left(\frac{\alpha_i(M_Z)}{\alpha_i(M_c)} \right)^{\frac{c_i^x}{2B_i}}.
\end{aligned} \tag{4.16}$$

The c^x and B govern the MSSM 1-loop running effects due to the gauge couplings:

$$\begin{aligned}
c^u &= \left(\frac{13}{15}, 3, \frac{16}{3} \right) \\
c^d &= \left(\frac{7}{15}, 3, \frac{16}{3} \right) \\
c^e &= \left(\frac{9}{5}, 3, 0 \right) \\
B &= \left(\frac{33}{5}, 1, -3 \right)
\end{aligned} \tag{4.17}$$

We estimate that the neglect of the running due to λ_b and λ_τ introduces 5% error in the down and charged lepton sectors and around 1% error in the up sector. We further estimate the neglect of 2-loop gauge running to be $\sim 1\%$ error in G_u and G_d , and $\sim 4\%$ error in G_e .

Because we use MSSM running from M_c down to M_Z , errors are introduced when we include particles in the running below their mass scales. These effects can be taken into account by weak-scale threshold corrections. However, in our analysis we do not keep track of the supersymmetric particle masses and so these corrections cannot be calculated. We can, nevertheless, estimate these effects. The SUSY thresholds for all of the down sector quarks were calculated in [50]. There are $\tan\beta$ -enhanced diagrams which contribute to m_b , m_s and m_d . Although the Higgsino contribution to the d , s threshold corrections are Yukawa-suppressed, the dominant correction comes from gluino and Wino loop diagrams which affect all three of these quarks equally (up to some small differences due to unequal squark masses). We therefore make the simplifying approximation that the SUSY threshold corrections for all of the down quarks are the same. The same approximation can be made separately for the up and charged lepton sectors where the differences in thresholds among the same particle type arise only from squark mass differences, and are small.

By assuming some range of SUSY parameters, Pierce et. al. [49] have estimated the SUSY threshold corrections to the 3rd family masses. Assuming a value of $\tan\beta \sim 30$ and $\mu > 0$, we estimate from plots in [49] the SUSY threshold effects (at m_t for top and M_Z for bottom and tau) in terms of % shifts and errors. The shifts for these particles, and by approximation the shifts for the 1st and 2nd family particles, are

$$\begin{aligned}
m_u, m_c, m_t & \quad (+2.0 \pm 3)\% & F_t \equiv 1.02 \\
m_d, m_s, m_b & \quad (-10.0 \pm 10)\% & F_b \equiv 0.90 \\
m_e, m_\mu, m_\tau & \quad (+1.5 \pm 2)\% & F_\tau \equiv 1.015.
\end{aligned}
\tag{4.18}$$

The factors F_x will be used to keep track of these corrections.

SUSY threshold corrections to the CKM matrix elements were also calculated in [50]. As those authors state, to a good approximation the only CKM elements which shift their sizes are $|V_{ub}|$, $|V_{cb}|$, $|V_{td}|$, and $|V_{ts}|$, and these shifts are the opposite of the chargino-induced shift in m_b . In addition, J shifts approximately twice the amount of the CKM elements. The contribution from charginos to the m_b shift is plotted separately in Pierce et. al. [49], and we estimate it to be $5 \pm 10\%$. For those CKM observables which have large SUSY threshold corrections:

$$\begin{aligned}
|V_{ub}|, |V_{cb}|, |V_{td}|, |V_{ts}| & \quad (-5.0 \pm 10)\% & F_V \equiv 0.95 \\
J & \quad (-10.0 \pm 20)\% & F_J \equiv 0.90.
\end{aligned}
\tag{4.19}$$

As explained in [50], each side of the unitarity triangle has one element which has a large SUSY threshold. This leads to the threshold for J , and also implies that the angles of the triangle are unaffected. Thus $\sin 2\beta$ does not get a correction. We assume that the correction to $|\varepsilon_K|$ is approximately the same size as the correction for J .

The mutual dependence of $y_t(m_t, M_c)$ and λ_t means that there is no simple analytic way of integrating to find $y_t(m_t, M_c)$. We choose, therefore, to fit $m_t(m_t)$ by adjusting $\lambda_t(M_c)$ and using the 1-loop equations with λ_t and g_i only to run down to m_t . The 1-loop RG equation is:

$$\frac{d\lambda_t}{dt} \simeq \frac{\lambda_t}{16\pi^2} \left[6\lambda_t^2 - \sum_i c_i^u g_i^2 \right] \quad (4.20)$$

with $t \equiv \log \mu$ where μ is the energy scale. The relation between the experimental value of $m_t(m_t)$ and $\lambda_t(m_t)$:

$$m_t(m_t) = \lambda_t(m_t) F_t \frac{v}{\sqrt{2}} \sin \beta \simeq \lambda_t(m_t) F_t \frac{v}{\sqrt{2}} \quad (4.21)$$

We have already assumed $\tan \beta \sim 30$, which means that $\sin \beta$ is negligible, and we have included the thresholds for $m_t(m_t)$ in the scale factor F_t .

The PS-breaking VEVs of χ^c and $\overline{\chi^c}$ are of order the cutoff scale. As in [20], we choose to parameterize these VEVs with a dimensionless parameter ζ_{brane} :

$$\langle \chi^c \rangle = \langle \overline{\chi^c} \rangle \equiv \sqrt{\frac{4M_*}{\pi g_5^2 \zeta_{\text{brane}}}} \quad (4.22)$$

Naive dimensional analysis leads to a value for ζ_{brane} :

$$\zeta_{\text{brane}} = 0.27 \quad (4.23)$$

Using this value and using the assumption of 5D gauge unification as in [20] with the 4D GUT scale inputs

$$\begin{aligned} M_G &= (2.5 \pm 0.5) \times 10^{16} \text{ GeV} \\ \alpha_{\text{GUT}} &= 1/(24 \pm 1) \\ \varepsilon_3 &= -0.035 \pm 0.005 \end{aligned} \quad (4.24)$$

leads to knowledge of M_* , M_c , and $\alpha_i(M_c)$:

$$\begin{aligned} M_* &= 2.3 \times 10^{17} \text{ GeV} \\ M_c &= 2.4 \times 10^{14} \text{ GeV} \\ \alpha_1(M_c) &= 0.035 \\ \alpha_2(M_c) &= 0.040 \\ \alpha_3(M_c) &= 0.044 \end{aligned} \quad (4.25)$$

The uncertainties in the 4D GUT scale parameters (especially α_{GUT}) introduce $\pm 9\%$ errors into G_u and G_d and $\pm 2\%$ error into G_e and y_t . The errors listed here on G_u and G_d have a high correlation and can be mostly neglected when considering ratios.

Considering all the sources of errors discussed above, we choose to parametrize our theoretical errors as $\pm 9\%$ G_u and G_d (with the errors highly correlated), $\pm 4.5\%$ on G_e , and $\pm 2\%$ on y_t . In addition, in our expressions, the masses themselves should have extra theoretical errors from both threshold corrections and the neglect of the contribution to Yukawa running due to λ_b and λ_τ . We choose the up-type quarks to have $\pm 3\%$ error, down-type $\pm 11\%$ error, and the charged leptons $\pm 5\%$. Each of these errors is correlated to some degree within each particle type.

Starting from the $\alpha_i(M_c)$ and using 1-loop running, we find the gauge coupling scale factors to be

$$\begin{aligned} G_u(M_Z, M_c) &= 0.33 \pm 0.03 \\ G_d(M_Z, M_c) &= 0.33 \pm 0.03 \\ G_e(M_Z, M_c) &= 0.70 \pm 0.03. \end{aligned} \tag{4.26}$$

Fitting the central value of $m_t(m_t) = 169 \pm 4 \text{ GeV}$, allowing for the m_t 1σ range, and including the 3% threshold error on the top quark leads to

$$\begin{aligned} \lambda_t(M_c) &= 0.59 \pm 0.12 \\ y_t(m_t, M_c) &= 0.903 \pm 0.018. \end{aligned} \tag{4.27}$$

We have included the 2% theoretical error on y_t .

We are now in a position to analyze our predictions. First, consider

$$\left(\frac{m_u}{m_c}\right) / \left(\frac{m_e}{m_\mu}\right) (M_c) \simeq \left(\frac{m_b}{m_\tau}\right) (M_c). \tag{4.28}$$

We choose to make a prediction for $\left(\frac{m_u}{m_c}\right) (M_Z)$. The prediction and corresponding experimental values are:

$$\begin{aligned} \left(\frac{m_u}{m_c}\right)_{\text{th}} (M_Z) &\simeq \left[\left(\frac{m_e}{m_\mu}\right) \left(\frac{m_b F_b G_d}{m_\tau F_\tau G_e y_t}\right) \right] (M_Z) \\ &\simeq 0.0037 \pm 0.0006 \\ \left(\frac{m_u}{m_c}\right)_{\text{exp}} (M_Z) &= 0.0023 \pm 0.0010 \end{aligned} \tag{4.29}$$

Our prediction falls outside of the experimental bounds and leads to a 1.2σ discrepancy with the data. Our model favors a larger value for $\left(\frac{m_u}{m_c}\right)$, indicating possibly a larger m_u and/or smaller m_c than currently measured.

Consider the second prediction:

$$m_d m_s m_b(M_c) = m_e m_\mu m_\tau(M_c) \quad (4.30)$$

After using the scale factors to get down to M_Z , this becomes

$$\begin{aligned} (m_d m_s m_b)_{\text{th}}(M_Z) &\simeq \left[(m_e m_\mu m_\tau) \frac{F_\tau^3 G_e^3}{F_b^3 G_d^3} y_t \right] (M_Z) \\ &\simeq (10.7 \pm 5.0) \times 10^5 \text{ MeV}^3 \\ (m_d m_s m_b)_{\text{exp}}(M_Z) &= (5.2 \pm 2.6) \times 10^5 \text{ MeV}^3. \end{aligned} \quad (4.31)$$

The uncertainty of 50% in the predicted value comes mostly from the 9% errors in the gauge running scale factors G_e and G_d and the 11% error associated with the down-type masses. The experimental error is dominated by the uncertainty in m_s (and hence m_d). The discrepancy in the two values is about 1σ , and we predict a slightly larger scale for the down-type masses than measured.

4.2 Numerical Fitting

Within this section we apply numerical methods to fit our model to the data. By using automated techniques, we can find all of the Yukawa parameters which fit the data, including those parameters which were difficult to determine analytically. We can also easily include 2-loop gauge running and (1-loop) running due to the whole Yukawa matrices, not just λ_t .

Our fitting procedure starts from the Yukawa matrix in equation (3.28) taken at the compactification scale. We determine the gauge couplings at that scale assuming unification and some usual values for the unification parameters as listed in equations (4.24). Using 2-loop gauge and 1-loop Yukawa MSSM running, the Yukawa matrices are run from the compactification scale down to M_Z and diagonalized to find the fermion masses and quark mixing angles. On the way to M_Z , the top running mass $m_t(m_t)$ and the running due to λ_t below m_t ($y_t(M_Z, m_t)$) are determined. The observables at M_Z are shifted by SUSY threshold effects, listed in equations (4.18) and (4.19). To counteract the inclusion of the incorrect top running between M_Z and m_t , we multiply the observables at M_Z by appropriate powers of $y_t(M_Z, m_t)$. The correct powers are determined from the scale factors listed in the previous section equations (4.14). The observables are then compared to data in a χ^2 function, which we minimize by altering the Yukawa input parameters.

The sources of error in this section are the following. First, as in the analytic section, the threshold effects on the observables at the weak scale due to the SUSY

Table 4: Observables used in the χ^2 analysis. The theoretical errors are combinations of estimates of weak threshold effects, GUT parameter uncertainties, and in the case of ε_K an additional theoretical uncertainty from B_K . All observables are at the M_Z energy scale, except for the top mass, which is at m_t .

Observable	Exp. Error %	Th. Error %	Total Error %	Value Used
Q	3.5	6.4	7.3	22.7 ± 1.7
m_c	23.1	3.6	23.4	0.73 ± 0.17 GeV
$m_t(m_t)$	2.4	3.2	4.0	169 ± 7 GeV
$\frac{m_s}{m_d}$	8.5	2.5	8.8	18.9 ± 1.7
$\frac{m_s}{m_b}$	24.8	2.2	24.9	0.0199 ± 0.0049
m_b	2.1	12.2	12.4	2.91 ± 0.36 GeV
$\frac{m_e}{m_\mu}$	0.0003	2.0	2.0	0.004738 ± 0.000095
$\frac{m_\mu}{m_\tau}$	0.02	2.0	2.0	0.0588 ± 0.0012
m_τ	0.02	2.0	2.0	1.747 ± 0.035 GeV
$ V_{us} $	1.6	0.0	1.6	0.2240 ± 0.0036
$ V_{cb} $	1.9	10.0	10.2	0.0415 ± 0.0042
$ V_{ub}/V_{cb} $	9.3	0.0	9.3	0.086 ± 0.008
$ V_{td} $	9.8	10.0	14.0	0.0082 ± 0.0011
$\sin 2\beta$	6.5	0.0	6.5	0.739 ± 0.048
$J \times 10^5$	10.0	20.0	22.4	3.0 ± 0.7
$ \varepsilon_K $	0.7	26.6	26.6	0.00228 ± 0.00061

particle spectrum are not calculated. We estimate these effects in the same way as in the previous section in equations (4.18) and (4.19). Second, the uncertainties in our canonical 4D GUT parameters still introduce theoretical errors in our low energy data. By altering these inputs and studying their effects on the calculated observables numerically, we estimate the theoretical errors on our observables from these effects. These estimates are in general a bit less than the errors assigned in the analytic section because some correlations are automatically included numerically which were not included before. Third, we have the usual experimental errors. We choose to combine errors in quadrature and assign a combined theoretical and experimental error to each observable. These observables and errors are listed in Table 4. Most theoretical errors cancel in the same-family mass ratios, up to a few percent. Hence, we have assigned a minimum 2% error on these ratios due to threshold effects. This is especially important

Table 5: Observables, target values, best fit values, and χ^2 contributions. All observables are at the M_Z energy scale, except for the top mass, which is at m_t .

Observable	Target Value	Fit Value	χ^2 Contribution
Q	22.7 ± 1.7	23.5	0.21
m_c	$0.73 \pm 0.17 \text{ GeV}$	0.59 GeV	0.67
$m_t(m_t)$	$169 \pm 7 \text{ GeV}$	167 GeV	0.11
$\frac{m_s}{m_d}$	18.9 ± 1.7	17.0	1.28
$\frac{m_s}{m_b}$	0.0199 ± 0.0049	0.0238	0.64
m_b	$2.91 \pm 0.36 \text{ GeV}$	2.46 GeV	1.57
$\frac{m_e}{m_\mu}$	0.004738 ± 0.000095	0.004729	0.01
$\frac{m_\mu}{m_\tau}$	0.0588 ± 0.0012	0.0588	0.00
m_τ	$1.747 \pm 0.035 \text{ GeV}$	1.757 GeV	0.08
$ V_{us} $	0.2240 ± 0.0036	0.2237	0.01
$ V_{cb} $	0.0415 ± 0.0042	0.0412	0.00
$ V_{ub}/V_{cb} $	0.086 ± 0.008	0.090	0.21
$ V_{td} $	0.0082 ± 0.0011	0.0084	0.03
$\sin 2\beta$	0.739 ± 0.048	0.720	0.15
$J \times 10^5$	3.0 ± 0.7	3.0	0.00
$ \varepsilon_K $	0.00228 ± 0.00061	0.00210	0.09
Total:			5.06

for the lepton ratios, whose experimental errors are negligible.

Taken from Martin and Vaughn [51], we use 2-loop gauge and 1-loop Yukawa renormalization group equations. As explained before, our boundary conditions are at M_c : Given a set of choices of the Yukawa parameters, we have the 3×3 complex Yukawa matrices at M_c ; with the assumption of gauge unification and with the 4D GUT parameters (equation (4.24)), we have $\alpha_i(M_c)$. Running due to the neutrino sector of the theory is neglected. We fit the 11 Yukawa parameters to the 16 observables listed in Table 4 by minimizing a χ^2 function

$$\chi^2 = \sum_{i=1}^N \frac{(X_{\text{Calc}}^i - X_{\text{Exp}}^i)^2}{(\sigma_X^i)^2}. \quad (4.32)$$

Our fit to the data is in Table 5 and the corresponding Yukawa parameters for this fit can be found in Table 6. A true χ^2 function assumes gaussian errors for its observables, something which we have implicitly assumed but which is not true for

Table 6: Minimum χ^2 fit Yukawa parameters.

Parameter	Value
ζ	2.152
α_0	0.0002007
β_0	0.003274
γ_0	0.02187
ε_0	0.0009816
c	1.492
θ_1	5.090
θ_2	2.718
κ	1.495
$\lambda_t(M_c)$	0.6057
$\tan \beta$	25.42

some of the observables used. Our χ^2 is more of an indication of how good the fit is, and the minimization of the function is a method by which we can find a “best” set of parameters for the fit. The fit value for our χ^2 is around 5, with the majority of the contribution coming from the down-type quark sector.

The value for m_u/m_c in the numerical fit (0.0040) is about 0.5σ away from the value found in the analytic section (0.0037 ± 0.0006), and is consistent with our prediction of a larger m_u and/or smaller m_c than measured. In addition, the best fit value for $m_d m_s m_b$ in the χ^2 analysis ($5.0 \times 10^5 \text{ MeV}^3$) is consistent with the value from the previous section ($(10.7 \pm 5.2) \times 10^5 \text{ MeV}^3$) (within 1.1σ) and with the measured value ($(5.2 \pm 2.6) \times 10^5 \text{ MeV}$). As for the free parameters, in the analytic section we fit only one of these: $\lambda_t(M_c) = 0.59 \pm 0.12$. The numerical fit value found here, 0.6057, falls well within the range of the analytic fit value. Thus, the results of the numerical (Section 4.2) and analytic (Section 4.1) analyses are consistent.

5. Justification in 6D

In this section we discuss a 6D version of our theory which naturally justifies our setup given in this paper. Our 5D analysis has assumed that the PS brane keeps its symmetry even though χ^c and $\bar{\chi}^c$ get their VEVs near the cutoff scale and break the PS symmetry entirely. As mentioned in section 3, there are generic large corrections in the Kahler

potentials of PS-brane fields ψ

$$K = (1 + C \frac{\chi^{c\dagger} \chi^c}{M_*^2}) \psi^\dagger \psi.$$

This problem can be solved in a geometric way by the addition of a sixth dimension along which χ^c and ψ are separated. Even for a tiny sixth dimension, $1/R_2 \sim M_*/3$, PS breaking effects are suppressed by e^{-3} which is enough suppression to keep our Yukawa relations. All of the numerical analysis given in the paper remains the same as long as the sixth dimension is not too large compared to the cutoff scale.

There are two distinct ways of constructing 6D models. First, a 6D N=1 (4D N=2) theory with T^2/Z_2 gives four fixed points (3+1 dimensional spacetime). All the fields in the bulk in the 5D theory are now in 6D in the 6D theory, while all the fields living on branes still live on branes. As we have one 10 dimensional hypermultiplet and two 16 dimensional hypermultiplets, we need one additional 16 dimensional hypermultiplet in order to cancel the 6D irreducible gauge anomaly of SO(10) [52].

Second, a 6D N=1 theory with $T^2/(Z_2 \times Z_2)$ also gives a 4D N=1 theory below the compactification scale. There are four fixed lines along $x^5 = 0, x^5 = \pi R_1/2, x^6 = 0,$ and $x^6 = \pi R_2/2$ and four fixed points at the corners. The gauge sector is extended to 6D, but all of the other bulk fields can still be on 5D fixed lines. This setup is anomaly free without introducing additional states.

Gauge coupling unification restricts the possible sizes of R_1 and R_2 in both cases. However, we can easily recover the 5D theory used in this paper in the limit $1/R_2 \rightarrow M_*$. Note, as long as $1/R_2$ is close to, but somewhat less than, M_* we simultaneously have gauge coupling unification (as described in the 5D formulation) and PS symmetry relations for Yukawa couplings.

We choose to focus on a 6D N=1 theory with T^2/Z_2 . Such a theory has been studied by Asaka, Buchmuller and Covi [19] where the SO(10) gauge group in the bulk is broken down to $SM \times U(1)_X$ by two different Wilson lines. One breaks SO(10) down to the Pati-Salam gauge group along x_5 , and the other breaks SO(10) down to $SU(5) \times U(1)_X$ along x_6 . Therefore, we end up with four fixed points; SO(10) brane at $(x_5, x_6) = (0, 0)$, Pati-Salam brane at $(\frac{\pi R_1}{2}, 0)$, Georgi-Glashow brane ($SU(5) \times U(1)_X$) at $(0, \frac{\pi R_2}{2})$ and flipped SU(5) brane ($SU(5)' \times U(1)'_X$) at $(\frac{\pi R_1}{2}, \frac{\pi R_2}{2})$. We have provided a schematic of the extra-dimensional space in Figure 1. The 5D setup we have considered so far can be easily lifted up to this configuration. The procedure is the following.

- 5D bulk states are extended to 6D bulk states. Extra hypermultiplets are introduced to cancel the 6D anomaly.
- Fields on the 5D SO(10) brane are located on the 6D SO(10) brane.

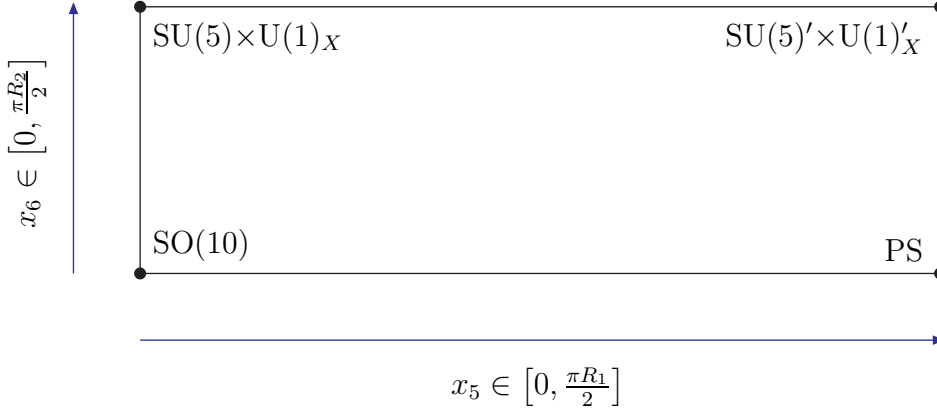


Figure 1: A representation of the 6D orbifold space. The orbifold fixed points are at the corners of the space. At each corner a different subgroup of $SO(10)$ is preserved. x_5 runs along the horizontal direction from 0 to $\frac{\pi R_1}{2}$, while x_6 runs along the vertical direction from 0 to $\frac{\pi R_2}{2}$.

- Fields on the 5D Pati-Salam brane are located on the 6D Pati-Salam brane except χ^c and $\bar{\chi}^c$. Note, in this framework we no longer need χ^c and $\bar{\chi}^c$, since the gauge group is broken down to $SU(3)_C \times SU(2)_L \times U(1)_Y \times U(1)_X$ by the two Wilson lines. Nevertheless, any PS breaking effects on the $SO(10)$ or PS branes, emanating from the PS breaking fixed points, are suppressed. $U(1)_X$ is broken near the compactification scale by 16_{kink} and $\bar{\chi}^c_{\text{kink}}$, the fields which generate the nonzero kink mass.

The 6D model is simple and economical. The additional states introduced to cancel the 6D anomaly are hypermultiplets and can become heavy by themselves. In addition they do not affect the differential running of the three gauge couplings. Let us focus on gauge coupling unification. The spectrum of massive Kaluza-Klein vector multiplets are given by

$$\begin{aligned}
 M_{++} &= \sqrt{\left(\frac{2n}{R_1}\right)^2 + \left(\frac{2m}{R_2}\right)^2} && (\text{SM} \times U(1)_X) \\
 M_{+-} &= \sqrt{\left(\frac{2n}{R_1}\right)^2 + \left(\frac{2m+1}{R_2}\right)^2} && \left(\frac{\text{PS}}{\text{SM} \times U(1)_X}\right) \\
 M_{-+} &= \sqrt{\left(\frac{2n+1}{R_1}\right)^2 + \left(\frac{2m}{R_2}\right)^2} && \left(\frac{\text{SU}(5)}{\text{SM}}\right)
 \end{aligned}$$

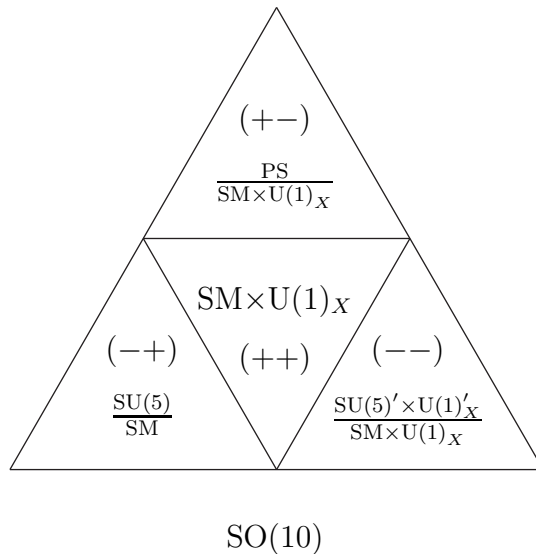


Figure 2: A representation of the SO(10) group space. The space has been broken into four subspaces by the orbifold symmetry, under which each subspace has a different parity.

$$M_{--} = \sqrt{\left(\frac{2n+1}{R_1}\right)^2 + \left(\frac{2m+1}{R_2}\right)^2} \left(\frac{\text{SU}(5)' \times \text{U}(1)'_X}{\text{SM} \times \text{U}(1)_X} \right).$$

The breakdown of SO(10) into these subgroups is illustrated in Figure 2. If we send $R_2 \rightarrow 0$, we recover a 5D theory in which $\text{SU}(5) \times \text{U}(1)_X$ is broken to the $\text{SM} \times \text{U}(1)_X$. The $R_2 \rightarrow 0$ limit gives the same result as in Hall and Nomura [13] (and also in Kim and Raby [20]). Thus we fix $M_c \sim 1/R_1$ at around 10^{14} GeV with $M_* \sim 10^{17}$ GeV. If $R_2 M_* \sim 2$ or 3 , we get a tiny correction from extra $-+$ states and the result would be proportional to $\frac{1}{3}(b_{\text{PS}} - b_{\text{SM}}) \log\left(\frac{R_2}{M_*}\right)$ which is negligibly small.¹¹ The elongated 6D rectangular configuration gives a perfect setup for the construction of a realistic SO(10) model.

The only remaining question is the applicability of bulk field localization in 6D which was possible with a kink mass in 5D. Though the quantitative results of 6D localization are different from the 5D case, all of the qualitative aspects remain the same [53]. More interestingly, 4D N=1 supersymmetry is preserved.

¹¹The notation used is defined in Kim and Raby [20].

6. Summary and Discussion

Extra dimensions provide a nice framework for understanding how grand unified theories may be realized in nature. In this paper we have constructed a 5D SO(10) model which accommodates the quark and charged lepton masses and the CKM matrix. The model uses 11 parameters to fit the 13 independent observables of the quark and charged lepton Yukawa sectors, allowing us to make two predictions: $\frac{m_u}{m_c}(M_Z) = 0.0037 \pm 0.0006$ and $m_d m_s m_b(M_Z) = (10.7 \pm 5.0) \times 10^5 \text{ MeV}^3$, both of which are roughly 1σ larger than the experimental values. The kink mass localizes the bulk Higgs fields according to their $U(1)_X$ quantum numbers, giving some explanation for the hierarchy $m_b \ll m_t$ and $m_d > m_u$. Our 5D SO(10) model can be considered to be an effective theory coming from 6D SO(10) with one small and one large extra dimension. If the size of the sixth dimension is very small (i.e. if the inverse of its characteristic length is near the cutoff scale) then all of the calculations done here for the 5D model can be regarded as good approximations for the 6D case.

In a theory in which there are additional (heavy) vector-like states, commonly called Froggatt-Nielsen (FN) fields, which have the same quantum numbers as the light states, the light and heavy states can mix. The extra dimension naturally gives us a chance to unify Froggatt-Nielsen fields with ordinary matter fields if both come from the same hypermultiplet in higher dimensions. In our model, however, we chose to place the 1st and 3rd family fields on opposite branes to easily take advantage of the effects of the kink mass, and so our model does not achieve the unification of the massless and FN states into bulk fields. Nevertheless, it may be possible to place all of the matter fields in the bulk and still restrict the Yukawa terms of those fields to opposite branes to gain the desired hierarchy from the kink mass. We leave this possibility for further research.

Further work is needed in six main areas in order to make our model complete. First, the neutrino sector should be included to explain neutrino oscillation experiments. We have already fixed the neutrino Dirac masses in terms of the Yukawa matrix between the left and right-handed neutrinos, but the heavy Majorana masses of the right-handed neutrinos have not yet been determined. It would be very interesting to expand the model to include Majorana masses and to investigate the resulting neutrino masses and mixings. Second, the weak scale supersymmetry breaking mechanism should be specified. As there is as yet no such universally accepted mechanism, we chose not to specify how SUSY is broken in our model. As a consequence, we could not calculate the electroweak threshold corrections resulting from superparticle spectrum. Extra dimensions provide new interesting channels for the understanding of supersymmetry breaking and its mediation and can give entirely different superparticle spectra. We leave the weak scale supersymmetry breaking physics to future work. Third, our

analysis is somewhat incomplete since we have taken values for α_{GUT} , M_G and ε_3 from other sources. Hence our treatment of gauge and Yukawa coupling RG running is not completely self consistent. We have however accounted for this shortcoming by including a theoretical uncertainty obtained by varying the gauge coupling parameters at M_G . While a more complete unification treatment would be preferable, this would require knowledge of supersymmetry breaking and the sparticle spectrum. Fourth, we have neglected the effects of running on the Yukawa matrices between the compactification and cutoff scales. Our assumption is that such effects would contribute at the level of a few percent. Further research is necessary to investigate these effects. Fifth, the UV completion of the higher dimensional gauge theory could give us a better understanding of the model. String theory does not allow arbitrary matter configurations and the constraints coming from it are usually stronger than those from field theory. Therefore, it would be interesting to see if the 5D model considered here can be derived as an effective field theory from a string theoretic starting point [54, 55]. Finally, we have assumed that many fields in our theory obtain vacuum expectation values at certain scales and in particular directions in group space. A complete theory would need to justify these VEVs by the minimization of the appropriate potentials. Such work would be most easily done after finding a successful UV completion for the theory, as many of these VEVs are of the order the cutoff energy scale.

Acknowledgments

We thank the Institute for Advanced Study School of Natural Sciences for their hospitality, and A. Falkowski for discussions on 5D orbifold propagators. Partial support for this work came from DOE grant# DOE/ER/01545-861.

Appendix

A. D_3 Family Symmetry

In this section, we define the D_3 group, give its character table, and give other information necessary to understand the couplings and representations used in our model. Our presentation is an abbreviation of a more complete description given in [32].

D_3 is the group of all rotations in three dimensions which leave an equilateral triangle invariant. The group contains six elements in three classes: E ; C_3 , C_3^2 ; C_a , C_b , C_c . E is the identity element. C_3 and C_3^2 signify 120° and 240° rotations about an axis through the center of and perpendicular to the triangle. C_a , C_b , and C_c signify 180° rotations about the three different axes which run from the center to the three

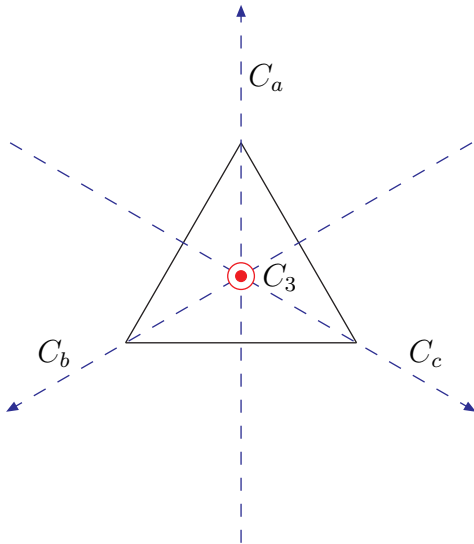


Figure 3: Graphic representation of our choice of D_3 group elements. The solid (black) lines represent the triangle. The 3 dashed (blue) lines represent the axes about which we take the C_a , C_b , and C_c rotations. The center (red) circle and dot represent the axis about which we take the C_3 rotation (it points out of the page). Our rotation convention is right-handed.

vertices of the triangle. We choose orientations such that $C_b = C_a C_3$ and $C_c = C_a C_3^2$. Figure 3 contains a graphic representation of our conventions for the group elements. The group has two inequivalent singlet representations: $\mathbf{1}_A$ and $\mathbf{1}_B$, and one doublet representation: $\mathbf{2}_A$.

The character table is

D_3	E	C_3	C_a
$\mathbf{1}_A$	1	1	1
$\mathbf{1}_B$	1	1	-1
$\mathbf{2}_A$	2	-1	0

(A.1)

We choose our representations as follows. When acting on a one dimensional representation, the elements are the characters in the character table. When acting on the two dimensional representation, the elements are

$$E = \begin{pmatrix} 1 & 0 \\ 0 & 1 \end{pmatrix} \quad C_3 = \begin{pmatrix} \epsilon & 0 \\ 0 & \epsilon^{-1} \end{pmatrix} \quad C_a = \begin{pmatrix} 0 & 1 \\ 1 & 0 \end{pmatrix}, \quad (\text{A.2})$$

with $\epsilon \equiv e^{2\pi i/3}$. The remaining elements can be found by group multiplication.

Our Lagrangian of Section 3.2 contains terms with various combinations of D_3 fields. It is understood that the Lagrangian only contains the D_3 singlet ($\mathbf{1}_A$) part of

these combinations. Here we list the combinations of fields we have used, and their singlet projections.

Let θ_i be $\mathbf{2}_A$ (doublet) fields under D_3 , and let the internal degrees of freedom be represented by x_i and y_i : $\theta_i \equiv \begin{pmatrix} x_i \\ y_i \end{pmatrix}$. Also, let ϕ be a $\mathbf{1}_B$ (“anti-symmetric” singlet) field, with internal degree of freedom α : $\phi \equiv \alpha$. Then the combinations we need are:

$$\begin{aligned} \theta_1 \times \theta_2|_{\mathbf{1}_A} &= x_1 y_2 + y_1 x_2 \\ \theta_1 \times \theta_2 \times \phi|_{\mathbf{1}_A} &= (x_1 y_2 - y_1 x_2) \alpha \\ \theta_1 \times \theta_2 \times \theta_3|_{\mathbf{1}_A} &= x_1 x_2 x_3 + y_1 y_2 y_3 \end{aligned} \tag{A.3}$$

Of course, multiplication by a “true” singlet $\mathbf{1}_A$ has no effect concerning the D_3 structure of the Lagrangian terms.

B. Massless States and Wavefunctions

This section will show how we determine the overlap between the original Lagrangian states and the massless states. We choose to illustrate this through a specific example: the determination of the overlap between the Lagrangian fields and the 3rd family left-handed states in equations (3.19) of section 3.2.

The relevant superpotential terms are (from equation (3.12)):

$$\begin{aligned} W_2 \supset (\bar{\psi}_{++})_a (\partial_y - m_X) (\psi_{--})_a \\ + [2\sigma\phi_a (\bar{\psi}_{++})_a \psi_3] \delta(y) + [2\eta (\bar{\psi}_{++})_a \chi_a] \delta(y - \frac{\pi R}{2}) \end{aligned} \tag{B.1}$$

The equations of motion are:

$$\begin{aligned} \frac{\partial W}{\partial (\bar{\psi}_{++})_a} = 0 \implies \\ 0 = (\partial_y - m_X) (\psi_{--})_a + 2\delta(y) \sigma \frac{\phi_a}{M_*} \sqrt{M_*} \psi_3 + 2\delta(y - \frac{\pi R}{2}) \eta \sqrt{M_*} \chi_a. \end{aligned} \tag{B.2}$$

We have added factors of M_* where necessary to ensure that we have unitless couplings σ and η . This equation is satisfied for the massless projections of these fields. Away from the branes, $(\psi_{--})_a \propto e^{m_X y}$. Because $(\psi_{--})_a$ is odd under both orbifold parities and because $e^{m_X y}$ is not an odd function about either $y = 0$ or $y = \frac{\pi R}{2}$, the profile of $(\psi_{--})_a$ must have discontinuities at both branes. These discontinuities can cancel the brane terms in the equations of motion. Define the overlap between ψ_3 and the

massless field ψ_3^0 as $\psi_3 \supset \tilde{n}_L \psi_3^0$. We can then solve for the other two fields:

$$\begin{aligned} (\psi_{--})_a &\supset -\varepsilon_{--}(y) e^{\frac{X_L \zeta y}{\pi R}} \left(\frac{\phi_a}{M_*} \right) \sigma \sqrt{M_*} \tilde{n}_L \psi_3^0 \\ \chi_a &\supset -e^{\frac{X_L \zeta}{2}} \left(\frac{\phi_a}{M_*} \right) \frac{\sigma}{\eta} \tilde{n}_L \psi_3^0 \end{aligned} \quad (\text{B.3})$$

What remains is to determine the normalization \tilde{n}_L . We do this by requiring that the effective 4D field ψ_3^0 have a canonical Kahler potential term. Listing the fields which contribute to this term (we have suppressed the gauge field factors here):

$$\begin{aligned} &\int_0^{\frac{\pi R}{2}} dy \left\{ \psi_3^\dagger \psi_3 \delta(y) + \sum_a (\psi_{--})_a^\dagger (\psi_{--})_a + \sum_a \chi_a^\dagger \chi_a \delta(y - \frac{\pi R}{2}) \right\} \\ &\supset \psi_3^{0\dagger} \psi_3^0 |\tilde{n}_L|^2 \left\{ 1 + \sum_a \left[\sigma^2 M_* \left(\frac{\phi_a}{M_*} \right)^2 \int_0^{\frac{\pi R}{2}} dy e^{\frac{2X_L \zeta y}{\pi R}} + \frac{\sigma^2}{\eta^2} \left(\frac{\phi_a}{M_*} \right)^2 e^{X_L \zeta} \right] \right\} \end{aligned} \quad (\text{B.4})$$

The integral is

$$\int_0^{\frac{\pi R}{2}} dy e^{\frac{2X_L \zeta y}{\pi R}} = \frac{1}{M_* \rho^2 n_L^2} \quad (\text{B.5})$$

which implies that for canonical normalization:

$$1 \equiv |\tilde{n}_L|^2 \left\{ 1 + \frac{\sigma^2}{\rho^2} \sum_a \left(\frac{\phi_a}{M_*} \right)^2 \left[\frac{1}{n_L^2} + \frac{\rho^2}{\eta^2} e^{X_L \zeta} \right] \right\}. \quad (\text{B.6})$$

Choose \tilde{n}_L to be real:

$$\tilde{n}_L \equiv \frac{1}{\sqrt{1 + r \left[\frac{1}{n_L^2} + \frac{\rho^2}{\eta^2} e^{X_L \zeta} \right]}} \quad (\text{B.7})$$

The other mixings and normalizations listed in Section 3.2 are calculated in the same way.

C. A Lifted 4D Model

We present here a 5D version of a 4D model by Dermisek and Raby in [32] which itself was based on prior works [56, 57, 58, 59]. Our purpose is to illustrate how such a 4D

model could be placed into a 5D context and what advantages can be gained from the use of the extra direction.

In using the extra dimension, we have separated the fields on the PS brane from the important mass parameter $M_\chi = M_0(1 + \alpha X)$ which gives much of the distinction between the particle types. There are matter fields on the PS brane, and bulk matter fields which mediate between these brane fields and the $\text{SO}(10)$ M_χ VEV in such a way to give us the desired Yukawa matrix elements.

The setup for this model is largely the same as that presented in Section 3, save for the following points. This model does not have a kink mass in the bulk; the small up quark mass comes instead from an approximate left-right symmetry in the model. Here we use a $B - L$ VEV on the PS brane instead of T_{3R} . Other differences lie in the placement of the matter fields and the extra VEV fields. As with the model presented in the main body of the paper, for the current model under discussion we also have in mind a setup which includes a small 6th dimension (as detailed in Section 5) in order to separate fields on the PS-brane from the PS-breaking VEVs. This allows us to preserve the PS Yukawa relations on the PS-brane below the cutoff scale.

The states are placed as follows. In the bulk, we have 8 matter hypermultiplets, forming 4 doublets under D_3 and transforming as 16s under $\text{SO}(10)$. Each of these hypermultiplet doublets has a different parity under the orbifold. The Higgs, as before, is contained inside a 10 hypermultiplet of $\text{SO}(10)$. These fields are listed in Table 7. On the $\text{SO}(10)$ brane there is only the mass parameter M_χ , which is a singlet under D_3 and is a mix of singlet and X under $\text{SO}(10)$: $M_\chi = \lambda_\chi \left(\frac{\chi^c \bar{\chi}^c}{M_*} \right) = M_0(1 + \alpha X)$. On the Pati-Salam brane, we have three sets of left- and right-handed matter fields. Two of these sets form a doublet under D_3 . In addition, there are several extra fields: $\phi_a, \tilde{\phi}_a, A, A_{15}, \Phi_L$, and Φ_R . Of these extra fields, those with subscript a are D_3 doublets. The rest are $\mathbf{1}_A$ save A which is $\mathbf{1}_B$ under D_3 . All of these extra fields get nonzero VEVs except for $\tilde{\phi}_1$. All extra fields are $\text{SO}(10)$ singlets, save A_{15} which is an $\text{SU}(4)$ adjoint and gets a VEV $\langle A_{15} \rangle = \langle A_{15}^0 \rangle (B - L)$. The PS brane fields are listed in Table 8.

We choose the following superpotential:

$$\begin{aligned}
W_1 &= \delta(y - \frac{\pi R}{2}) \left\{ \lambda_1 \psi_3 H \psi_3^c + \lambda_2 \psi_a H (\psi_{++}')_a \Phi_R + \lambda_2 (\psi_{++})_a H \psi_a^c \Phi_L \right\} \quad (\text{C.1}) \\
W_2 &= \overline{16}_a \partial_y 16_a + \overline{16}'_a \partial_y 16'_a + \overline{16}_a \partial_y \tilde{16}_a + \overline{16}'_a \partial_y \tilde{16}'_a + \overline{10} \partial_y 10 \\
&\quad + \delta(y) \left\{ M_\chi \overline{16}_a 16'_a + M_\chi \overline{16}'_a 16_a \right\} \\
&\quad + \delta(y - \frac{\pi R}{2}) \left\{ \left(\overline{\psi}'_{++} \right)_a \left[\lambda_3 A_{15} \phi_a \psi_3 + \lambda_4 A_{15} \tilde{\phi}_a \psi_a + \lambda_5 A \psi_a \right] \Phi_L \right. \\
&\quad \left. + \left(\overline{\psi}^c_{++} \right)_a \left[\lambda_3 A_{15} \phi_a \psi_3^c + \lambda_4 A_{15} \tilde{\phi}_a \psi_a^c + \lambda_5 A \psi_a^c \right] \Phi_R \right\}
\end{aligned}$$

Table 7: Bulk fields

Field	PS Symm	D_3 Symm
$16 = \begin{pmatrix} \psi_{++} \\ \psi_{+-}^c \end{pmatrix}$	$\begin{pmatrix} (4, 2, 1) \\ (\bar{4}, 1, 2) \end{pmatrix}$	$\mathbf{2}_A$
$\overline{16} = \begin{pmatrix} \overline{\psi}_{--} \\ \overline{\psi}_{-+}^c \end{pmatrix}$	$\begin{pmatrix} (\bar{4}, 2, 1) \\ (4, 1, 2) \end{pmatrix}$	$\mathbf{2}_A$
$16' = \begin{pmatrix} \psi'_{+-} \\ \psi'_{++}{}^c \end{pmatrix}$	$\begin{pmatrix} (4, 2, 1) \\ (\bar{4}, 1, 2) \end{pmatrix}$	$\mathbf{2}_A$
$\overline{16}' = \begin{pmatrix} \overline{\psi}'_{-+} \\ \overline{\psi}'_{--}{}^c \end{pmatrix}$	$\begin{pmatrix} (\bar{4}, 2, 1) \\ (4, 1, 2) \end{pmatrix}$	$\mathbf{2}_A$
$\widetilde{16} = \begin{pmatrix} \widetilde{\psi}_{-+} \\ \widetilde{\psi}_{--}^c \end{pmatrix}$	$\begin{pmatrix} (4, 2, 1) \\ (\bar{4}, 1, 2) \end{pmatrix}$	$\mathbf{2}_A$
$\overline{\widetilde{16}} = \begin{pmatrix} \overline{\widetilde{\psi}}_{+-} \\ \overline{\widetilde{\psi}}_{++}^c \end{pmatrix}$	$\begin{pmatrix} (\bar{4}, 2, 1) \\ (4, 1, 2) \end{pmatrix}$	$\mathbf{2}_A$
$\widetilde{16}' = \begin{pmatrix} \widetilde{\psi}'_{--} \\ \widetilde{\psi}'_{-+}{}^c \end{pmatrix}$	$\begin{pmatrix} (4, 2, 1) \\ (\bar{4}, 1, 2) \end{pmatrix}$	$\mathbf{2}_A$
$\overline{\widetilde{16}'} = \begin{pmatrix} \overline{\widetilde{\psi}}'_{++} \\ \overline{\widetilde{\psi}}'_{+-}{}^c \end{pmatrix}$	$\begin{pmatrix} (\bar{4}, 2, 1) \\ (4, 1, 2) \end{pmatrix}$	$\mathbf{2}_A$
$10 = \begin{pmatrix} H_{++} \\ H_{+-}^c \end{pmatrix}$	$\begin{pmatrix} (1, 2, 2) \\ (6, 1, 1) \end{pmatrix}$	$\mathbf{1}_A$
$\overline{10} = \begin{pmatrix} \overline{H}_{--} \\ \overline{H}_{-+}^c \end{pmatrix}$	$\begin{pmatrix} (1, 2, 2) \\ (6, 1, 1) \end{pmatrix}$	$\mathbf{1}_A$

There are 12 $U(1)$ symmetries associated with our superpotential. We choose to parametrize these by allowing the following 12 fields to be charged each under different $U(1)$ s: $\psi_3, \psi_3^c, H_{+-}^c, M_\chi, \left(\widetilde{\psi}'_{--}\right)_a, \left(\widetilde{\psi}'_{-+}\right)_a, \left(\widetilde{\psi}_{-+}\right)_a, \Phi_L, A_{15}$. After specifying the $U(1)$ symmetries of the above fields, the $U(1)$ transformations of all other fields are uniquely defined. There are in addition 2 Z_2 symmetries. First is the Z_2 orbifold parity under $y \rightarrow -y$. The transformations of the bulk fields under this symmetry have already been defined. In addition, let the rest of the independent fields: $\psi_3, \psi_3^c, M_\chi, \Phi_L, A_{15}$ be even under this symmetry. The second Z_2 involves a sign ambiguity in the transformation of Φ_R . Under a given symmetry, if $\Phi_L \rightarrow e^{i\alpha}\Phi_L$, then the superpotential terms imply that $\Phi_R \rightarrow e^{in\pi}e^{i\alpha}\Phi_R$ with $n = 0, 1$. We choose to require that $n = 1$ here

Table 8: PS Brane fields

Field	PS Symm	D_3 Symm
ψ	$(4, 2, 1)$	$\mathbf{2}_A$
ψ^c	$(\bar{4}, 1, 2)$	$\mathbf{2}_A$
ψ_3	$(4, 2, 1)$	$\mathbf{1}_A$
ψ_3^c	$(\bar{4}, 1, 2)$	$\mathbf{1}_A$
ϕ	$(1, 1, 1)$	$\mathbf{2}_A$
$\tilde{\phi}$	$(1, 1, 1)$	$\mathbf{2}_A$
A	$(1, 1, 1)$	$\mathbf{1}_B$
A_{15}	$(1, 1, 3)$	$\mathbf{1}_A$
Φ_L	$(1, 1, 1)$	$\mathbf{1}_A$
Φ_R	$(1, 1, 1)$	$\mathbf{1}_A$

in order to forbid terms created by the replacement of Φ_L by Φ_R or vice-versa. We also assume that $\langle \Phi_L \rangle / M_* \ll 1$ so that replacements like $\Phi_L \rightarrow \Phi_R^2$ are negligible.¹² Let the 12 independent fields be uncharged under this symmetry. We require all of these symmetries just listed to be symmetries of the theory so as to forbid unwanted extra terms in the superpotential.

The superpotential has a left-right symmetry, under which $\psi_3 \leftrightarrow \psi_3^c$, $\psi \leftrightarrow \psi^c$, $\left(\frac{16}{\bar{16}}\right) \leftrightarrow \left(\frac{16'}{\bar{16}'}\right)$, $\left(\frac{\tilde{16}}{\tilde{16}}\right) \leftrightarrow \left(\frac{\tilde{16}'}{\tilde{16}'}\right)$, $\Phi_L \leftrightarrow \Phi_R$. This symmetry, which commutes with the family D_3 symmetry, is broken spontaneously by the VEVs of Φ_L and Φ_R , which we require to be slightly different. This difference is encapsulated by a small parameter η : $\langle \Phi_R \rangle = \langle \Phi_L \rangle (1 + \eta)$.

We now turn to the equations of motion for the left-handed states:

$$\begin{aligned}
 \frac{\partial W}{\partial_y (\bar{\psi}_{--})_a} = 0 &\implies \partial_y (\psi_{++})_a = 0 & (C.2) \\
 \frac{\partial W}{\partial_y (\bar{\psi}'_{-+})_a} = 0 &\implies \partial_y (\psi'_{+-})_a = 0 \\
 \frac{\partial W}{\partial_y (\bar{\tilde{\psi}}_{+-})_a} = 0 &\implies \partial_y (\tilde{\psi}_{-+})_a + \delta(y) M_\chi (\psi'_{+-})_a = 0
 \end{aligned}$$

¹²Such terms given by the substitution $\Phi_L \rightarrow \Phi_R^2$ or $\Phi_R \rightarrow \Phi_L^2$ would lead to a Yukawa matrix structure different from the one desired and so should be forbidden by some symmetry.

$$\begin{aligned}
\frac{\partial W}{\partial y \left(\tilde{\psi}'_{++} \right)_1} = 0 &\implies \partial_y \left(\tilde{\psi}'_{--} \right)_2 + \delta(y) M_\chi (\psi_{++})_2 \\
&\quad + \delta\left(y - \frac{\pi R}{2}\right) \left[\lambda_3 A_{15} \phi_2 \psi_3 + \lambda_4 A_{15} \tilde{\phi}_1 \psi_1 + \lambda_5 A \psi_2 \right] \Phi_L = 0 \\
\frac{\partial W}{\partial y \left(\tilde{\psi}'_{++} \right)_2} = 0 &\implies \partial_y \left(\tilde{\psi}'_{--} \right)_1 + \delta(y) M_\chi (\psi_{++})_1 \\
&\quad + \delta\left(y - \frac{\pi R}{2}\right) \left[\lambda_3 A_{15} \phi_1 \psi_3 + \lambda_4 A_{15} \tilde{\phi}_2 \psi_2 - \lambda_5 A \psi_1 \right] \Phi_L = 0
\end{aligned}$$

Solving these equations leads to knowledge of the overlap between the massless fields and the original fields in the Lagrangian. The following relationships only have the massless components on the right hand sides of the equations. (We have replaced the brane fields by their VEVs)

$$\begin{aligned}
(\psi'_{+-})_a &\supset 0 & (C.3) \\
(\tilde{\psi}_{-+})_a &\supset 0 \\
\left(\tilde{\psi}'_{--} \right)_1 &\supset \frac{1}{2} \tilde{\varepsilon}(y) \left[\lambda_3 \langle A_{15} \rangle \langle \phi_1 \rangle \psi_3 + \lambda_4 \langle A_{15} \rangle \langle \tilde{\phi}_2 \rangle \psi_2 - \lambda_5 \langle A \rangle \psi_1 \right] \langle \Phi_L \rangle \\
\left(\tilde{\psi}'_{--} \right)_2 &\supset \frac{1}{2} \tilde{\varepsilon}(y) \left[\lambda_3 \langle A_{15} \rangle \langle \phi_2 \rangle \psi_3 + \lambda_5 \langle A \rangle \psi_2 \right] \langle \Phi_L \rangle \\
(\psi_{++})_1 &\supset -\frac{1}{M_\chi} \left[\lambda_3 \langle A_{15} \rangle \langle \phi_1 \rangle \psi_3 + \lambda_4 \langle A_{15} \rangle \langle \tilde{\phi}_2 \rangle \psi_2 - \lambda_5 \langle A \rangle \psi_1 \right] \langle \Phi_L \rangle \\
(\psi_{++})_2 &\supset -\frac{1}{M_\chi} \left[\lambda_3 \langle A_{15} \rangle \langle \phi_2 \rangle \psi_3 + \lambda_5 \langle A \rangle \psi_2 \right] \langle \Phi_L \rangle
\end{aligned}$$

The equations for the right-handed states can be obtained from the left-right symmetry present in the model. We list the most important of these equations:

$$\begin{aligned}
(\psi^c_{++})_1 &\supset -\frac{1}{M_\chi} \left[\lambda_3 \langle A_{15} \rangle \langle \phi_1 \rangle \psi_3^c + \lambda_4 \langle A_{15} \rangle \langle \tilde{\phi}_2 \rangle \psi_2^c - \lambda_5 \langle A \rangle \psi_1^c \right] \langle \Phi_R \rangle & (C.4) \\
(\psi^c_{++})_2 &\supset -\frac{1}{M_\chi} \left[\lambda_3 \langle A_{15} \rangle \langle \phi_2 \rangle \psi_3^c + \lambda_5 \langle A \rangle \psi_2^c \right] \langle \Phi_R \rangle
\end{aligned}$$

The three ψ_i fields span the space of the left-handed massless states. Because the other fields which we've integrated out have massless components, the kinetic energy and gauge interaction terms for the ψ_i fields are no longer orthonormal. The same is true for the ψ_i^c states by the left-right symmetry. We will discuss the effects of rotating and rescaling these fields to an orthonormal basis later.

We replace the $(\psi_{++})_a$ and $(\psi'_{++})_a$ fields in W_1 by their corresponding massless parts in order to get the low energy Yukawa matrices. The result:¹³

$$\begin{aligned}
Y_u &= \begin{pmatrix} 0 & \varepsilon'\rho & r\varepsilon\kappa T_{uc} \\ -\varepsilon'\rho & \varepsilon\rho & r\varepsilon T_{uc} \\ r\varepsilon\kappa T_Q & r\varepsilon T_Q & 1 \end{pmatrix} \lambda \\
Y_d &= \begin{pmatrix} 0 & \varepsilon' & r\varepsilon\sigma\kappa T_{dc} \\ -\varepsilon' & \varepsilon & r\varepsilon\sigma T_{dc} \\ r\varepsilon\kappa T_Q & r\varepsilon T_Q & 1 \end{pmatrix} \lambda \\
Y_e &= \begin{pmatrix} 0 & -\varepsilon' & r\varepsilon\kappa T_{ec} \\ \varepsilon' & 3\varepsilon & r\varepsilon T_{ec} \\ r\varepsilon\sigma\kappa T_L & r\varepsilon\sigma T_L & 1 \end{pmatrix} \lambda
\end{aligned} \tag{C.5}$$

Definitions follow for these variables, where we have used $M_\chi = M_0(1 + \alpha X)$, $\langle\Phi_R\rangle = \langle\Phi_L\rangle(1 + \eta)$, and have added factors of the cutoff scale in order to make the couplings λ_i all unitless. We have also assumed $\eta \ll 1$ and $\alpha \sim \mathcal{O}(1)$. T_f represents the $(B - L)$ quantum number for the field f .

$$\begin{aligned}
\varepsilon &\equiv \frac{\lambda_2\lambda_4\langle A_{15}^0\rangle\langle\tilde{\phi}_2\rangle\langle\Phi_L\rangle^2}{3\lambda_1M_*^3M_0} \frac{4\alpha}{(1+\alpha)(1-3\alpha)} \\
\varepsilon' &\equiv -\frac{\lambda_2\lambda_5\langle A\rangle\langle\Phi_L\rangle^2}{\lambda_1M_*^2M_0} \frac{4\alpha}{(1+\alpha)(1-3\alpha)} \\
\rho &\equiv \frac{2\eta(1-3\alpha)}{4\alpha} \\
r &\equiv -\frac{\lambda_3\langle\phi_1\rangle}{\lambda_4\langle\tilde{\phi}_2\rangle} \frac{3(1-3\alpha)}{4\alpha} \\
\kappa &\equiv \frac{\langle\phi_2\rangle}{\langle\phi_1\rangle} \\
\sigma &\equiv \frac{1+\alpha}{1-3\alpha} \\
\lambda &\equiv \lambda_1\sqrt{\frac{2M_c}{\pi M_*}}
\end{aligned} \tag{C.6}$$

These Yukawa matrices are the same as those found in [32], except for the (1,3) and (3,1) elements. It has been shown in [46] that (1,3) elements are needed in models of this kind in order to fit $\sin 2\beta$.

¹³We have chosen to use the notation found in [32] to ease comparison between prior works and our own.

Here we list the lowest-order diagrams which give the Yukawa matrices. Each diagram is followed by the element(s) to which it contributes.

$$\begin{array}{c}
H \downarrow \\
\hline
\psi_3 \qquad \psi_3^c
\end{array} \tag{3,3}$$

$$\begin{array}{c}
H \downarrow \quad \Phi_R \quad M_\chi \quad A_{15} \downarrow \quad \phi_a \quad \Phi_R \\
\hline
\psi_a \quad (\psi_{++}^c)_a \quad (\widetilde{\psi}_{++}^c)_a \quad \psi_3^c
\end{array} \tag{1,3} \tag{2,3}$$

$$\begin{array}{c}
A_{15} \downarrow \quad \phi_a \quad \Phi_L \quad M_\chi \quad H \downarrow \quad \Phi_L \\
\hline
\psi_3 \quad (\widetilde{\psi}'_{++})_a \quad (\psi_{++})_a \quad \psi_a^c
\end{array} \tag{3,1} \tag{3,2}$$

$$\begin{array}{c}
H \downarrow \quad \Phi_R \quad M_\chi \quad A_{15} \downarrow \quad \widetilde{\phi}_a \quad \Phi_R \\
\hline
\psi_a \quad (\psi_{++}^c)_a \quad (\widetilde{\psi}_{++}^c)_a \quad \psi_a^c
\end{array} \tag{2,2}$$

$$\begin{array}{c}
A_{15} \downarrow \quad \widetilde{\phi}_a \quad \Phi_L \quad M_\chi \quad H \downarrow \quad \Phi_L \\
\hline
\psi_a \quad (\widetilde{\psi}'_{++})_a \quad (\psi_{++})_a \quad \psi_a^c
\end{array} \tag{2,2}$$

$$\begin{array}{c}
H \downarrow \quad \Phi_R \quad M_\chi \quad A \downarrow \quad \Phi_R \\
\hline
\psi_a \quad (\psi_{++}^c)_a \quad (\widetilde{\psi}_{++}^c)_a \quad \psi_a^c
\end{array} \tag{1,2} \tag{2,1}$$

$$\begin{array}{c}
A \downarrow \quad \Phi_L \quad M_\chi \quad H \downarrow \quad \Phi_L \\
\hline
\psi_a \quad (\widetilde{\psi}'_{++})_a \quad (\psi_{++})_a \quad \psi_a^c
\end{array} \tag{1,2} \tag{2,1}$$

We performed a χ^2 analysis, the same as that used in [56], save that here we have nonzero (1,3) and (3,1) terms and a new parameter κ . The fit parameters follow.

First the GUT parameters:

$$\begin{aligned}
\frac{1}{\alpha_{\text{GUT}}} &= 25.12 & (\text{C.7}) \\
M_G &= 2.54 \times 10^{16} \text{ GeV} \\
\varepsilon_3 &= -3.61\%
\end{aligned}$$

Next the (modulus) Yukawa sector:

$$\begin{aligned}
\lambda &= 0.70 & (\text{C.8}) \\
r &= 24.8 \\
\sigma &= 1.19 \\
\varepsilon &= 0.0090 \\
\rho &= 0.061 \\
\varepsilon' &= 0.0034 \\
\kappa &= 0.15
\end{aligned}$$

Next the Yukawa phase information ($\phi_x \equiv \arg(x)$) in radians:

$$\begin{aligned}
\phi_\sigma &= 0.51 & (\text{C.9}) \\
\phi_\rho &= -1.87 \\
\phi_\kappa &= 0.89
\end{aligned}$$

The other Yukawa parameters are assumed to be real. Finally some SUSY breaking scales and $\tan\beta$:

$$\begin{aligned}
\mu &= 234 \text{ GeV} & (\text{C.10}) \\
M_{1/2} &= 606 \text{ GeV} \\
m_{16} &= 4160 \text{ GeV} \\
A_0 &= -7736 \text{ GeV} \\
\left(\frac{m_{10}}{m_{16}}\right)^2 &= 1.80 \\
\left(\frac{m_D}{m_{16}}\right)^2 &= 0.128 \\
\tan\beta &= 52.2
\end{aligned}$$

The fit itself can be found in Table 9. As explained in Section 4.2, we are using our χ^2 function as a vehicle to find the best possible fit rather than as a true statistical

Table 9: Best fit. Mass dimensions are in GeV.

Observable	Target Value	Fit Value	χ^2 Contribution
$\frac{1}{\alpha_{\text{EM}}}$	137.04 ± 0.14	137.0	0.08
$G_\mu \times 10^5$	1.1664 ± 0.0012	1.166	0.11
α_s	0.1172 ± 0.0020	0.1167	0.06
M_{Top}	178.0 ± 4.3	176.5	0.12
m_b	4.220 ± 0.090	4.243	0.07
$M_b - M_c$	3.40 ± 0.20	3.35	0.06
m_s	0.089 ± 0.011	0.104	1.86
$\frac{1}{Q^2} \times 10^3$	2.03 ± 0.20	2.00	0.02
$\frac{m_d}{m_s}$	0.050 ± 0.015	0.074	2.54
M_τ	1.7770 ± 0.0018	1.777	0.00
M_μ	0.10566 ± 0.00011	0.1057	0.13
$M_e \times 10^3$	0.51100 ± 0.00051	0.5110	0.00
V_{us}	0.2230 ± 0.0040	0.2216	0.12
V_{cb}	0.0402 ± 0.0019	0.0390	0.40
$\frac{V_{ub}}{V_{cb}}$	0.0860 ± 0.0080	0.0863	0.00
$\varepsilon_K \times 10^3$	2.28 ± 0.23	2.35	0.10
M_Z	91.188 ± 0.091	91.19	0.00
M_W	80.419 ± 0.080	80.41	0.01
m_c	1.30 ± 0.15	1.15	1.00
$(b \rightarrow s\gamma) \times 10^3$	0.334 ± 0.038	0.335	0.00
$\sin 2\beta$	0.727 ± 0.036	0.700	0.57
$V_{td} \times 10^3$	8.20 ± 0.82	8.35	0.03
		Total:	7.30

χ^2 function. Our best χ^2 is 7.30, indicating that we are not fitting some of the data. Specifically, as shown in Table 9, the observables m_s , $\frac{m_d}{m_s}$, and m_c have χ^2 contributions of 1 or greater and make up the majority of the χ^2 fit value. The fit values of the down and strange quark masses are on the large side, while the charm mass fit value is smaller than the data. We present this fit as a first attempt at this kind of model. More work is needed to alter the model to obtain a better fit.

In our analysis we have used a basis in which the massless matter fields are not orthonormal. Rotation and rescaling to a canonical orthonormal basis would in general introduce changes to the Yukawa matrices. We have neglected effects from this change of basis, and our justification for this is the following. Were a fit to be done with these

effects included, the input Yukawa parameters would compensate by changing their values. We assume that the input parameters could compensate to the extent that we would obtain essentially the same fit in this case as in the case we have presented here in the appendix without these extra effects. We leave it to further research to explore whether this assumption is a good one.

References

- [1] S. Dimopoulos, S. Raby and F. Wilczek, Phys. Rev. D **24**, 1681 (1981).
- [2] S. Dimopoulos and H. Georgi, Nucl. Phys. B **193**, 150 (1981).
- [3] L. E. Ibanez and G. G. Ross, Phys. Lett. B **105**, 439 (1981).
- [4] N. Sakai, Z. Phys. C **11**, 153 (1981).
- [5] M. B. Einhorn and D. R. T. Jones, Nucl. Phys. B **196**, 475 (1982).
- [6] W. J. Marciano and G. Senjanovic, Phys. Rev. D **25**, 3092 (1982).
- [7] S. Raby, Phys. Rev. D **66**, 010001 (2002).
- [8] H. Georgi and C. Jarlskog, Phys. Lett. B **86**, 297 (1979).
- [9] Y. Kawamura, Prog. Theor. Phys. **105**, 999 (2001) [arXiv:hep-ph/0012125].
- [10] Y. Kawamura, Prog. Theor. Phys. **105**, 691 (2001) [arXiv:hep-ph/0012352].
- [11] G. Altarelli and F. Feruglio, Phys. Lett. B **511**, 257 (2001) [arXiv:hep-ph/0102301].
- [12] L. J. Hall and Y. Nomura, Phys. Rev. D **64**, 055003 (2001) [arXiv:hep-ph/0103125].
- [13] L. J. Hall and Y. Nomura, Phys. Rev. D **65**, 125012 (2002) [arXiv:hep-ph/0111068].
- [14] L. J. Hall and Y. Nomura, Phys. Rev. D **66**, 075004 (2002) [arXiv:hep-ph/0205067].
- [15] A. B. Kobakhidze, Phys. Lett. B **514**, 131 (2001) [arXiv:hep-ph/0102323].
- [16] A. Hebecker and J. March-Russell, Nucl. Phys. B **613**, 3 (2001) [arXiv:hep-ph/0106166].
- [17] A. Hebecker and J. March-Russell, Nucl. Phys. B **625**, 128 (2002) [arXiv:hep-ph/0107039].
- [18] R. Dermisek and A. Mafi, Phys. Rev. D **65**, 055002 (2002) [arXiv:hep-ph/0108139].
- [19] T. Asaka, W. Buchmuller and L. Covi, Phys. Lett. B **523**, 199 (2001) [arXiv:hep-ph/0108021].

- [20] H. D. Kim and S. Raby, *JHEP* **0301**, 056 (2003) [arXiv:hep-ph/0212348].
- [21] S. B. Giddings and A. Strominger, *Nucl. Phys. B* **307**, 854 (1988).
- [22] S. R. Coleman, *Nucl. Phys. B* **310**, 643 (1988).
- [23] G. Gilbert, *Nucl. Phys. B* **328**, 159 (1989).
- [24] Y. Kawamura, H. Murayama and M. Yamaguchi, *Phys. Rev. D* **51**, 1337 (1995) [arXiv:hep-ph/9406245].
- [25] K. S. Babu and R. N. Mohapatra, *Phys. Rev. Lett.* **83**, 2522 (1999) [arXiv:hep-ph/9906271].
- [26] L. M. Krauss and F. Wilczek, *Phys. Rev. Lett.* **62**, 1221 (1989).
- [27] C. H. Albright, *Int. J. Mod. Phys. A* **18**, 3947 (2003) [arXiv:hep-ph/0212090].
- [28] M. C. Chen and K. T. Mahanthappa, *Int. J. Mod. Phys. A* **18**, 5819 (2003) [arXiv:hep-ph/0305088].
- [29] G. Altarelli and F. Feruglio, arXiv:hep-ph/0405048.
- [30] N. Arkani-Hamed and M. Schmaltz, *Phys. Rev. D* **61**, 033005 (2000) [arXiv:hep-ph/9903417].
- [31] H. D. Kim, J. E. Kim and H. M. Lee, *Eur. Phys. J. C* **24**, 159 (2002) [arXiv:hep-ph/0112094].
- [32] R. Dermisek and S. Raby, *Phys. Rev. D* **62**, 015007 (2000) [arXiv:hep-ph/9911275].
- [33] M. Battaglia *et al.*, arXiv:hep-ph/0304132.
- [34] A. Hocker, H. Lacker, S. Laplace and F. Le Diberder, *Eur. Phys. J. C* **21**, 225 (2001) [arXiv:hep-ph/0104062]. For updated Lepton-Photon 2003 result, see: http://www.slac.stanford.edu/laplace/ckmfitter/ckm_results_summer03.html.
- [35] K. Hagiwara *et al.* [Particle Data Group Collaboration], *Phys. Rev. D* **66**, 010001 (2002).
- [36] H. Leutwyler, *Phys. Lett. B* **378**, 313 (1996) [arXiv:hep-ph/9602366].
- [37] R. Gupta and K. Maltman, *Int. J. Mod. Phys. A* **16S1B**, 591 (2001) [arXiv:hep-ph/0101132].
- [38] C. W. Bauer, Z. Ligeti, M. Luke and A. V. Manohar, *Phys. Rev. D* **67**, 054012 (2003) [arXiv:hep-ph/0210027].

- [39] P. Azzi *et al.* [CDF Collaboration], arXiv:hep-ex/0404010.
- [40] H. Fusaoka and Y. Koide, Phys. Rev. D **57**, 3986 (1998) [arXiv:hep-ph/9712201].
- [41] T. Inami and C. S. Lim, Prog. Theor. Phys. **65**, 297 (1981) [Erratum-ibid. **65**, 1772 (1981)].
- [42] N. Arkani-Hamed, T. Gregoire and J. Wacker, JHEP **0203**, 055 (2002) [arXiv:hep-th/0101233].
- [43] R. Kitano and T. j. Li, Phys. Rev. D **67**, 116004 (2003) [arXiv:hep-ph/0302073].
- [44] H. Murayama and A. Pierce, Phys. Rev. D **65**, 055009 (2002) [arXiv:hep-ph/0108104].
- [45] L. J. Hall and A. Rasin, Phys. Lett. B **315**, 164 (1993) [arXiv:hep-ph/9303303].
- [46] H. D. Kim, S. Raby and L. Schradin, Phys. Rev. D **69**, 092002 (2004) [arXiv:hep-ph/0401169].
- [47] S. M. Barr and I. Dorsner, Phys. Lett. B **556**, 185 (2003) [arXiv:hep-ph/0211346].
- [48] V. D. Barger, M. S. Berger and P. Ohmann, Phys. Rev. D **47**, 2038 (1993) [arXiv:hep-ph/9210260].
- [49] D. M. Pierce, J. A. Bagger, K. T. Matchev and R. j. Zhang, Nucl. Phys. B **491**, 3 (1997) [arXiv:hep-ph/9606211].
- [50] T. Blazek, S. Raby and S. Pokorski, Phys. Rev. D **52**, 4151 (1995) [arXiv:hep-ph/9504364].
- [51] S. P. Martin and M. T. Vaughn, Phys. Rev. D **50**, 2282 (1994) [arXiv:hep-ph/9311340].
- [52] T. Asaka, W. Buchmuller and L. Covi, Nucl. Phys. B **648**, 231 (2003) [arXiv:hep-ph/0209144].
- [53] H. M. Lee, H. P. Nilles and M. Zucker, Nucl. Phys. B **680**, 177 (2004) [arXiv:hep-th/0309195].
- [54] T. Kobayashi, S. Raby and R. J. Zhang, arXiv:hep-ph/0403065.
- [55] T. Kobayashi, S. Raby and R. J. Zhang, “Searching for realistic 4d string models with a Pati-Salam symmetry: Orbifold arXiv:hep-ph/0409098.
- [56] T. Blazek, S. Raby and K. Tobe, Phys. Rev. D **60**, 113001 (1999) [arXiv:hep-ph/9903340].
- [57] R. Barbieri, L. J. Hall and A. Romanino, Phys. Lett. B **401**, 47 (1997) [arXiv:hep-ph/9702315].

- [58] R. Barbieri, L. J. Hall, S. Raby and A. Romanino, Nucl. Phys. B **493**, 3 (1997)
[arXiv:hep-ph/9610449].
- [59] T. Blazek, M. Carena, S. Raby and C. E. M. Wagner, Phys. Rev. D **56**, 6919 (1997)
[arXiv:hep-ph/9611217].